Modeling Conformance as Dispersion

K.H. Coats, Coats Engineering; **C.H. Whitson,** Norwegian University of Science and Technology (NTNU AND PERA); and **L.K. Thomas,** Consultant

Summary

For decades the effect of physical dispersion (in-situ mixing) in porous media has been of interest in reservoir engineering and groundwater hydrology. Dispersion can affect the development of multicontact miscibility and bank breakdown in enriched-gas drives and miscible solvent floods of any mobility ratio.

The magnitude or extent of dispersion is quantified by the rock property physical dispersivity, α, which is on the order of 0.01 ft for consolidated rocks and several times smaller for sandpacks, as found in many laboratory measurements.

Numerical studies of the effect of dispersion on enriched-gas drives and field tracer tests often use input values of a scale-dependent dispersivity 100 to 1,000 or more times larger than $\approx$0.01 ft. These large scale-dependent dispersivity values stem from large apparent dispersivities (α_a) determined by matching the 1D convection/diffusion (C/D) equation to production-well-effluent tracer-concentration profiles observed in field tracer tests.

A scale-dependent dispersivity can be used only as a fitting factor to match or explain the effluent profile of a single producer at a fixed distance from an injector. It cannot represent physical dispersion to justify the conclusions reached by its use in simulations of enriched-gas-drive, field-tracer-test, or other reservoir displacement processes. It has no predictive value in any numerical simulation.

The scale-dependent apparent dispersivities reflect conformance or other behavior not governed by the 1D C/D equation and should not be used to justify large dispersivities as input to numerical studies. This paper shows that large apparent dispersivities observed in field tests can result with physical dispersivity no larger than the $\approx$0.01-ft laboratory-measured value.

Heterogeneity alone (no physical dispersivity or molecular diffusion) causes no in-situ mixing and cannot explain observed large apparent echo-test dispersivities. Large apparent dispersivities for two reported echo (single-well inject/produce) tracer tests are shown to result from a model with drift alone and no dispersion.

The widely reported scale dependence of apparent dispersivity is a simple and necessary consequence of mis-applying the 1D C/D equation, with its single parameter of Peclet number, L/α, to conformance it does not describe. The conformance portion, α_{ac}, of apparent dispersivity, α_a, is scale-dependent, but physical dispersivity is a rock property independent of scale and time. The value of α_a approximately obeys an additive dispersivity principle, $\alpha_a \approx \alpha + \alpha_{ac}$, where α_{ac} is dispersivity representing conformance and $\alpha_{ac} >> \alpha$ in field displacements.

Introduction

This paper differentiates between the rock-property physical dispersivity, α, associated with dispersion (in-situ mixing), and apparent dispersivity, α_a, associated with conformance. Apparent dispersivities, α_a, are determined by a best-fit match of the 1D C/D equation to effluent-concentration profiles, C, vs. pore volumes injected, Q_D, from field tracer tests or numerical simulations. For the assumptions used in this paper, conformance reflects the combined effects of heterogeneity, well areal pattern, well-completion intervals, and drift (regional flow gradient).

The α_a values derived from field-tracer-test data appear to be strongly scale-dependent (Arya et al. 1988; Mahadevan et al. 2003) with log-log plots of α_a vs. scale, L, showing a slope of roughly 1. Field-scale α_a values are orders of magnitude larger than laboratory-measured dispersivities (Perkins and Johnston 1963), $\alpha \approx 0.01$ ft, which have no scale dependence.

Our concern, and the reason for this paper, is the use of large scale-dependent apparent-dispersivity values as input dispersivity in numerical studies (Mahadevan et al. 2003; Todd and Chase 1979; Solano et al. 2001; Stalkup 1998; Johns et al. 2000; Shrivastava 2002) designed to quantify the impact of dispersion on reservoir processes. (These reservoir processes include solvent floods and enriched-gas drives of any mobility ratio, tracer tests, bank or slug breakdown, and chemical reactions.) The studies referred to use input dispersivity values as large as 8,000 times larger than a physical dispersivity $\approx$0.01 ft. More than 40 years ago, Mercado (Mercado 1967) showed that large apparent dispersivities from transmission (two-well) field tracer tests reflected conformance (heterogeneity) not dispersion. We argue that dispersivity $\approx$0.01 ft should be entered in fine-grid mechanistic studies designed to quantify the impact of physical dispersion on reservoir processes.

We show in this paper that apparent dispersivities are approximately the sum of physical dispersivity, α, and apparent dispersivity owing only to conformance, α_{ac}, $\alpha_a \approx \alpha + \alpha_{ac}$. For field-scale cases of practical interest, $\alpha_{ac} >> \alpha$, which makes $\alpha_a \approx \alpha_{ac}$ an excellent approximation. We also show that $\alpha_{ac} \approx \alpha_{ap} + \alpha_{as}$, where α_{ap} is the apparent dispersivity owing to pattern (areal) sweep alone, and α_{as} is the apparent dispersivity resulting from stratification (vertical) sweep alone.

The literature gives considerable attention to the scale dependence of apparent dispersivities. We show that this is a necessary and expected consequence of matching the 1D C/D equation—the single parameter in this equation is the Peclet number $N_{Pe} = L/\alpha$—which describes dispersion, to effluent-concentration profiles, which reflect conformance. With very few exceptions, there is no physical meaning or significance to this scale dependence.

Some authors state or imply that heterogeneity causes in-situ mixing (Mahadevan et al. 2003; Stalkup 1998; Kossack 1989). We argue that heterogeneity alone ($\alpha = \alpha_t = D_0 = 0$) causes no in-situ mixing—a fact we believe has been a long-recognized tenet of reservoir engineering.

Several studies (Arya et al. 1988; Kossack 1989; Warren and Skiba 1981) use zero input dispersivities when numerically simulating heterogeneous systems for the purpose of generating apparent dispersivities. These results reflect only conformance and any numerical dispersion present. The magnitude of the generated apparent dispersivities, their scale-dependence, and their relation to heterogeneities have nothing to do with dispersion or physical dispersivity; heterogeneity alone causes no in-situ mixing.

Numerical-simulation results were reported recently (Mahadevan et al. 2003) for echo and transmission tests that can be interpreted with large, scale-dependent apparent dispersivity, α_a, and large "local" dispersivities determined from gridblock $C(t)$ profiles. We show that these results are influenced by numerical dispersion. We also show that these results illustrate the additive-dispersivity approximation.

Large apparent dispersivities observed in field echo (single-well) tests (Pickens and Grisak 1981) up to 3 ft have yet to be explained in the literature by use of a physical model. We show that large α_a values in echo tests can result from natural drift and/or transverse dispersion in laminations with contrasting permeabilities.

Assumptions, Definitions, and Methods

Except where otherwise noted, assumptions in this paper are as follows. We consider unit-mobility-ratio displacements in a

This paper (SPE 90390) was accepted for presentation at the SPE Annual Technical Conference and Exhibition, Houston, 26–29 September 2004, and revised for publication. Original manuscript received for review 7 June 2007. Revised manuscript received for review 6 March 2008. Paper peer approved 27 September 2008.

porous medium of any heterogeneity, dimensionality, and geometry. Injected (displacing) and original (displaced) fluids have equal viscosities and densities, are incompressible, and obey the law of additive volumes. Wells are vertical and fully penetrating. Darcy flow and uniform porosity and formation thickness are assumed. These displacements include—on laboratory or field scale—tracer tests and first-contact miscible (solvent) floods. Effects of tracer adsorption and degradation are neglected.

We begin with some key definitions. We also describe methods for modeling laboratory and field tests designed to measure physical dispersivity and/or conformance.

Concentration and Effluent Profile. For field tracer tests, concentration, C, is tracer concentration normalized by initial injected-tracer concentration. For miscible solvent floods, C is the fraction of solvent in solvent/oil mixtures. Effluent profile or profile is the production wellstream, C, vs. time or pore volumes injected resulting from an injection process.

A clear distinction should be made between in-situ and effluent concentrations. Mixing in the reservoir is associated with in-situ concentrations. Mixing in the wellbore and surface facilities is associated with wellstream-effluent concentration [a weighted average of flowing concentrations (Johns et al. 2000)].

Physical Dispersion. The terms physical dispersion and dispersion are used interchangeably to denote the in-situ mixing attributable to dispersion coefficients (Perkins and Johnston 1963), K_ℓ and K_t (Eq. 5), in the presence of flow and/or concentration gradients. In modeling, in-situ mixing should not occur if these coefficients are entered as zero.

Physical Dispersivity. Physical dispersivity, α, is a rock property determined from flow tests by use of laboratory core plugs or sandpacks, which are homogeneous or nearly so. The terms physical dispersivity and dispersivity are used interchangeably. Two dispersivities exist (relative to flow direction): longitudinal, α, and transverse, α_t. Dispersivity is a *microstructural (Mercado 1967)* rock property related to irregularities in pore structure at the level of pore dimensions (microscale heterogeneity). Physical dispersivity is neither time-dependent nor scale-dependent, regardless of whether scale is defined as system length, distance traveled, or "scale of heterogeneity."

Perkins and Johnston (1963) give an "average" longitudinal $\alpha = 0.006$ ft (0.18 cm) for sandstones and transverse α_t that is 30 times less; they give significantly smaller α values for unconsolidated sand. Others report laboratory-measured dispersivities $\approx$0.01 ft and transverse dispersivities some 10 to 100 times less.

C/D Equations. For a 1D miscible displacement in a homogeneous porous medium, the concentration profile in time and distance is given by (Aronofsky and Heller 1957)

$$C = \frac{1}{2} erfc\left(\frac{x_D - Q_D}{2\sqrt{Q_D/N_{Pe}}}\right) + \frac{e^{x_D N_{Pe}}}{2} erfc\left(\frac{x_D + Q_D}{2\sqrt{Q_D/N_{Pe}}}\right), \quad \ldots (1)$$

where $erfc$ is the complimentary error function, $erfc(a) = 1 - erf(a)$; x_D is the dimensionless distance traveled, x/L; Q_D is the dimensionless pore volumes injected; and N_{Pe} is the dimensionless Peclet number given by $N_{Pe} = uL/K_\ell$. Defining longitudinal dispersivity, $\alpha = K_\ell / u$, where K_ℓ is the longitudinal dispersion coefficient, gives

$$\alpha = \frac{1}{N_{Pe}} L. \quad \ldots (2)$$

Considering the effluent concentration profile at $x = L$ ($x_D = 1$), we can rewrite Eq. 1 as

$$C = \frac{1}{2} erfc\left(\frac{1 - Q_D}{2\sqrt{Q_D/N_{Pe}}}\right) + \frac{e^{N_{Pe}}}{2} erfc\left(\frac{1 + Q_D}{2\sqrt{Q_D/N_{Pe}}}\right), \quad \ldots (3)$$

or the more familiar simplified C/D equation by use of only the first term:

$$C = \frac{1}{2} erfc\left(\frac{1 - Q_D}{2\sqrt{Q_D/N_{Pe}}}\right), \quad \ldots (4)$$

which can be used for $N_{Pe} > 35$. Perkins and Johnston (1963) give

$$K_l = D^* + \alpha u$$
$$K_t = D^* + \alpha_t u, \quad \ldots (5)$$

where $D^* = D_0/\tau$; D_0 is the molecular diffusion coefficient, on the order of 10^{-5} cm^2/s for liquid/liquid systems; and τ is tortuosity, approximately 1.5 to 2.

Apparent Dispersivity. Apparent dispersivity, α_a, is determined by a best-fit match of the C/D transport term to effluent profile, C, vs. Q_D data from a field tracer test or numerical simulation. Most often the 1D C/D equation is used to fit $C(Q_D)$ data directly, where apparent Peclet number N_{Pea} is the fitting parameter, $\alpha_a = L/N_{Pea}$.

Best-Fit Procedure. Our approach to fitting the C/D equation, Eq. 3, to effluent profiles minimizes a least-squares function, f,

$$f(N_{Pe}) = \sum (\Delta C_i)^2, \quad \ldots (6)$$

ΔC_i is a residual defined as the difference in C/D-model C and the C "data" being fit. Usually all data are fit, but sometimes data are included for only a limited range of Q_D.

The only model parameter is Peclet number N_{Pe}. The α_a must be calculated from the best-fit N_{Pea} ($= \phi L/\alpha_a$) by use of scale L equal to "distance traveled." For a transmission (two-well) test, L is interwell distance.

For an echo (single-well) test, L is twice the mean depth of penetration L_m (Pickens and Grisak 1981). For an x-z cross section, L_m is calculated from $qt = \phi w H L_m$, where q is injection rate and t is time at the end of injection. For the field echo test, L_m is calculated from $qt = \pi \phi H L_m^2$.

Conformance. Conformance is usually considered to consist of two components: areal sweep and vertical sweep. Muskat (Muskat 1949) shows analytically that the two components of sweep can be treated individually and composited thereafter, as illustrated in Appendix A. Conformance reflects the combined effects of heterogeneity, well areal pattern and completion intervals, and drift.

Well-Pattern Areal Sweep. Areal conformance is dictated by well placement in an areal pattern. Analytical solutions exist for the homogeneous five-spot and two-spot patterns. The confined five-spot solution (Morel-Seytoux 1965) is:

$$Q_D = 0.457 K(90C), \quad \ldots (7)$$

where $K(x)$ is the complete elliptic integral of the first kind with x in degrees. Breakthrough time for the five spot is $Q_{DBT} = 0.7178$.

The unconfined two-spot solution (Hagoort 1982) is:

$$Q_D = \frac{1 - \pi C/\tan(\pi C)}{\sin^2(\pi C)}, \quad \ldots (8)$$

where pore volume is defined as $\phi \pi H d^2$, and d is the distance between wells. Breakthrough occurs at $Q_{DBT} = 1/3$.

Stratification. A stratified formation is defined as one where permeability varies only with z. Examples are the linear, exponential, and log-normal $k(z)$ described by Muskat (Muskat 1949). Also, discrete layers of different permeabilities and thicknesses represent a stratified formation. If formation thickness is constant and wells are fully penetrating, there is no crossflow (vertical flow between layers) in a stratified formation, and vertical permability is irrelevant.

The Muskat model for exponential $k(z)$ is given by

$$K(z) = k_{\min} e^{bz/H}, \quad \ldots\ldots\ldots\ldots\ldots\ldots\ldots\ldots\ldots\ldots (9)$$

where $k_{\max} = k_{\min} e^{b}$. Muskat further defines the ratio $r = k_{\max}/k_{\min}$. The Muskat model for linear $k(z)$ is given by

$$K(z) = k_{\min}[1 + (r-1)z/H], \quad \ldots\ldots\ldots\ldots\ldots\ldots\ldots\ldots (10)$$

where, again, $r = k_{\max}/k_{\min}$. The log-normal distribution of $k(z)$, as given by Muskat, is

$$\mathrm{d}z/\mathrm{d}\Psi = \frac{H}{\sigma\sqrt{2\pi}} e^{-\Psi^2/2\sigma^2}, \quad \ldots\ldots\ldots\ldots\ldots\ldots\ldots\ldots (11)$$

where $\Psi = \ln(k/k_{\min})$.

The Dykstra-Parsons V parameter (Dykstra and Parsons 1950) is related to the log-normal standard deviation, σ, by the relation $\sigma = -ln(1-V)$, or $V = 1 - \mathrm{e}^{-\sigma}$.

Heterogeneity. Heterogeneity (macroscale) indicates spatial variation in rock properties, mainly permeability $k(x,y,z)$ and porosity. Homogeneity, the opposite, implies uniform or spatially invariant rock properties. Stratification is an example of heterogeneity in the z-direction with homogeneity in the x-and y-directions, $k = k(z)$. Unless otherwise stated, the term heterogeneity denotes macroscale heterogeneity.

Variation *V*. V is the Dykstra-Parsons variation (1950), characterizing the degree of macroscale heterogeneity. It is 0 for a homogeneous porous medium (the microscale heterogeneity of pore dimensions is ever-present) and increases to 1.0 for the highest degree of heterogeneity.

Muskat Analytical Model. Muskat (1949) gave an analytical solution for the effect of any stratification $k(z)$ on effluent profile, $C(Q_D)$, for any areal geometry and well pattern with no vertical crossflow and negligible transverse dispersion. His solution is useful in examining and explaining the magnitude and scale dependence of apparent dispersivities derived from tracer tests. Let the base function, F, be defined as the concentration-profile response for a vertically homogeneous system. His analytical solution is

$$C(Q_D) = \frac{\int_0^H F(Q_{Dz})\, k(z)\, \mathrm{d}z}{\bar{k} H}, \quad \ldots\ldots\ldots\ldots\ldots\ldots\ldots\ldots (12)$$

where:

$$Q_{Dz} = \frac{k(z)}{k} Q_D, \quad \ldots\ldots\ldots\ldots\ldots\ldots\ldots\ldots\ldots\ldots (13)$$

$$\bar{k} = \frac{\int_0^H k(z)\, \mathrm{d}z}{H}, \quad \ldots\ldots\ldots\ldots\ldots\ldots\ldots\ldots\ldots\ldots (14)$$

and F is any function giving concentration vs. pore volumes injected for the vertically homogeneous system. Example base functions, $F(Q_D)$, are the analytical five-spot (Morel-Seytoux 1965) and two-spot (Hagoort 1982) solutions (α=0), the step function from 0 to 1 at Q_D=1 for the linear drive (100% areal conformance) with α=0, and the C/D equation (Eq. 3) for the linear drive with any α>0. Analytical $F(Q_D)$ solutions are not available for areal well patterns including longitudinal physical dispersion. If such solutions can be determined by other means then they can be used in Eq. 12.

Muskat gives analytical integrations of his Eq. 12 for the exponential, linear, and log-normal probability stratifications $k(z)$ of Eqs. 9 through 11 above. He shows that $C(Q_D)$ is dependent only upon the single parameter $r = k_{\max}/k_{\min}$ for the exponential and linear $k(z)$ and only upon V for the log-normal $k(z)$. The $k(z)$ function can be continuous or can be a step function representing any number of layers of any permeabilities and thicknesses. The ordering of $k(z)$ is irrelevant. For the three $k(z)$ stratifications just mentioned and for any given $k(z_D)$, $C(Q_D)$ is independent of both H and scale, L, if $\alpha = 0$. Muskat notes that the linear $k(z)$ case may be a reasonable approximation in some cases if permeabilities from logs and core plugs are rearranged in monotonically increasing order.

Single-Well (Echo) Test. A single-well test, also referred to as an echo test, involves the injection of a tracer with constant concentration into a single well, followed by production from the same well. Well-effluent concentrations are measured during the production period.

Traditional interpretation of an echo test uses the linear or radial C/D equation, neglecting any regional flow field that might exist during the test. The radial C/D equation proposed by Gelhar and Collins (Gelhar and Collins 1971) can be shown to be "equivalent" to the simplified one-term linear C/D equation (Eq. 4) for linear-model Peclet number $N_{PeL} > 20$, if we use the relation $N_{PeL} = 6N_{PeR}$, where $N_{PeR} = L/\alpha$ and $L = 2L_m$.

Two-Well (Transmission) Test. A two-well test, also referred to as a transmission test, involves the continuous or slug injection of a tracer into one well with production from a second well. Effluent concentrations are measured from the production well. In a recirculating two-well test, a tracer slug is injected followed by injection of produced water containing its tracer concentrations.

Drift (Regional Flow Gradient). In practically all groundwater systems and in petroleum reservoirs with an active flood, a regional flow gradient ("drift") exists where the tracer test is conducted (Tomich et al. 1973; Wellington et al. 1994). Interference of the natural linear velocity field and the test-well radial velocity field changes the otherwise circular shape of the injected tracer front to a distorted ellipse. For an echo test, the resulting smeared effluent profile will have an associated apparent dispersivity $\alpha_a > \alpha$. Most references in the literature tend to ignore the effect of drift on test results.

We present simulation results indicating that drift provides a physical explanation for large apparent dispersivities reported for the single- and two-well tests of Pickens and Grisak (1981).

Numerical Modeling Well-Effluent Concentrations. In this study we used three numerical models: (1) SENSOR (Coats Engineering; Marco Island, Florida; 2004), a finite-difference simulator that uses single-point upstream weighting; (2) UTCHEM (University of Texas; Austin, Texas; 1998), a finite-difference simulator that uses true vertical depth higher-order difference scheme; and (3) 3DSL (SteamSim Technologies; San Francisco; 2004), a streamline simulator.

Heterogeneity Alone Causes No In-Situ Mixing

We use the terms heterogeneity alone, conformance alone, and purely convective interchangeably, meaning that diffusion and convective dispersion are 0 (K_ℓ and K_t of Eq. 5 are 0). Heterogeneity alone causes no in-situ mixing. For $K_\ell = K_t = 0$, the transport equation is hyperbolic, containing first-order terms $u_x \partial C/\partial x$, $u_y \partial C/\partial y$, $u_z \partial C/\partial z$ but no second-order terms of Fickian type $K\partial^2 C/\partial x^2$. As a consequence, the displacement front is piston-like with no transition zone.

To illustrate, consider a 2D heterogeneous five spot with a 7×7 checkerboard description. The red squares (on the diagonals) are 100 md and 0.2 porosity, and the black squares are 1 md and 0.1 porosity. **Fig. 1** shows a concentration contour map at 0.3366 pore volumes injected, calculated by use of the 3DSL streamline model with a 567×567 grid and 3,688 streamlines. The displacement front is piston-like; there are no concentrations between 0 and 1.

However, the effluent profile shown in **Fig. 2** is smeared, reflecting conformance caused by the severe heterogeneity. The system has an apparent Peclet number of 2.71 (poor-quality fit), with an apparent dispersivity $\alpha_a = L/2.71$. This α_a is a "conformance index" bearing no relation to in-situ mixing in the reservoir. The Peclet number of 2.71 compares with an apparent Peclet

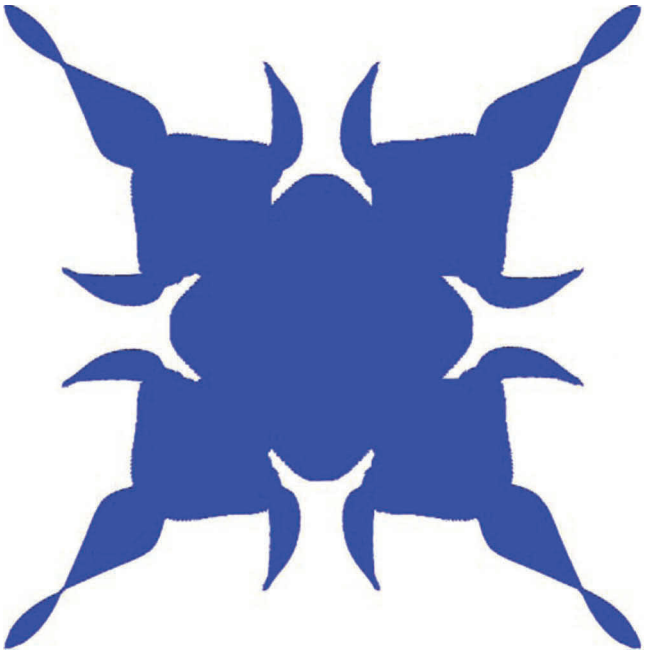

Fig. 1—Concentration profile (blue=1, white=0) from 3DSL streamline simulation at Q_D=0.3366 with single-layer 7 × 7 checkerboard five-spot pattern with 100:1 permeability ratio and 2:1 porosity ratio in alternating 7 × 7 square regions (high-k and high-ϕ squares at corners).

number of 18 for the homogeneous five-spot case. On a log-log plot of α_a vs. scale, L, both this heterogeneous case and the homogeneous case exhibit scale-dependent (parallel) lines of slope 1, but the heterogeneous α_a values are approximately seven times larger at any L. Recall that physical dispersivity, α, is zero for both of these cases. Heterogeneity alone causes smeared effluent curves and large, scale-dependent apparent dispersivities. But it does not cause in-situ mixing.

Single-well tracer tests give echo apparent dispersivities up to 3 ft or larger (Stalkup 1998; Pickens and Grisak 1981). Several authors state that these echo apparent dispersivities should approximate physical dispersivity in stratified formations where crossflow is absent (Mahadevan et al. 2003; Stalkup 1998; Pickens and Grisak 1981), provided effects of transverse dispersion between adjacent thin layers are negligible. But this should also be true in formations of arbitrary heterogeneity with crossflow if drift is zero or negligible. For zero K_ℓ and K_t, a streamline model will calculate a diverging piston-like displacement front during injection. The stream lines do not change with time, and the shape of the front will reflect the formation heterogeneity. Upon initiation of production, all points on the displacement front will retreat toward the well, arriving at the same time, giving a step-function effluent profile. Thus, heterogeneity alone (of any type in the absence of drift) cannot be considered the reason for observed apparent echo dispersivities 10 to 100 or more times larger than laboratory-measured $\alpha \approx 0.01$ ft.

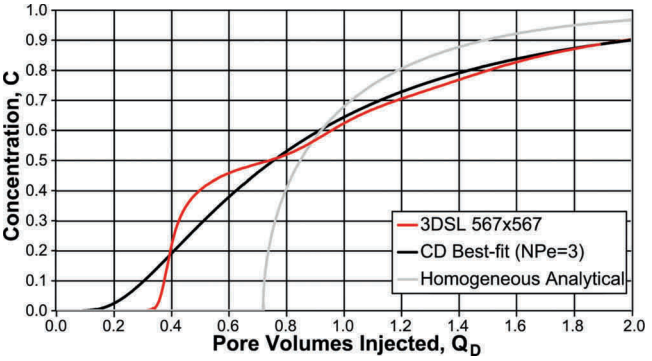

Fig. 2—Single-layer checkerboard five-spot by use of stream line numerical simulator 3DSL (red line). Best-fit to the CD Eq. 3 with apparent Peclet numbers N_{Pea}=3 (black line). Comparison with single-layer homogeneous five-spot (gray line).

Scale Dependence of Apparent Dispersivity

Plots of apparent dispersivity vs. scale (Arya et al. 1988; Mahadevan et al. 2003) (travel length) L show a near-linear dependence, though scatter is significant.

An acceptable explanation for this linear scale dependence is not readily found in the literature, apart from Mercado's work (Mercado 1967), which is sometimes referenced but seldom pursued. Physical dispersivity associated with in-situ mixing is known to be invariant with travel distance, so the explanation must lie elsewhere.

In this paper, we show that the scale dependence of apparent dispersivity, when it exists, is a natural and expected consequence of the fact that apparent dispersivities reflect conformance, not physical dispersion.

Five Spot. We start with the simple example of a homogeneous five spot. The analytical solution equation (Eq. 7) gives a unique function $C(Q_D)$. A fit of this profile to the C/D equation (Eq. 3) gives a best fit (for $0<Q_D<2$) apparent conformance Peclet number of $N_{Pea}=N_{Peap}=18$. This corresponds to a scale-dependent apparent dispersivity of

$$\alpha_a = \frac{1}{N_{Pea}}L = \frac{1}{18}L = 0.056L$$

Fig. 3 shows the best fit of this solution. **Fig. 4** shows the resulting plot of α_a vs. L superimposed on literature-reported apparent dispersivities.

Two Spot. Next we consider a homogeneous two spot. The analytical solution Eq. 8 gives a unique function $C(Q_D)$. A fit of this profile to the CD Eq. 3 gives a best fit (for $0<Q_D<2$) apparent conformance Peclet number of $N_{Pea}=N_{Peap}=3$. This corresponds to a scale-dependent apparent dispersivity of:

$$\alpha_a = \frac{1}{3}L = 0.33L$$

Fig. 3 shows the best-fit of this solution. The fit is not good for $Q_D>0.8$ and is increasingly poor for $Q_D>1$; depending on the range of Q_D, the best-fit apparent Peclet number will vary. Fig. 4 shows the resulting plot of α_a vs. L for a two spot with $N_{Pea}=3$.

The two-spot solution is the expected performance of a two-well transmission test (in the absence of drift). Some authors correctly interpret transmission profiles with a two-spot flow model (Pickens and Grisak 1981) but still require apparent

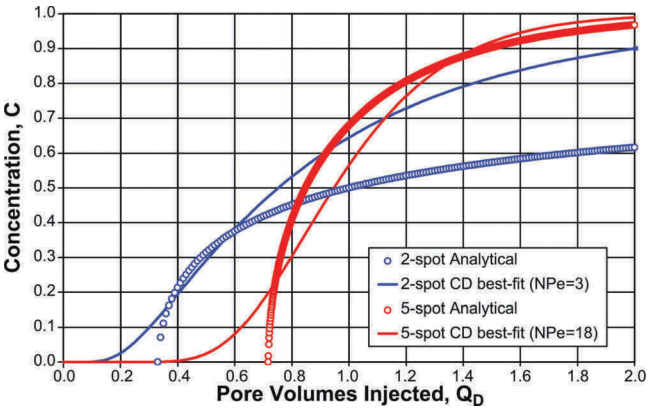

Fig. 3—Single-layer two-spot and five-spot $C(Q_D)$ profiles from analtytical solutions. Best fit to the CD Eq. 3 with apparent Peclet numbers N_{Pea}=3 and 18, respectively. Zero physical dispersion.

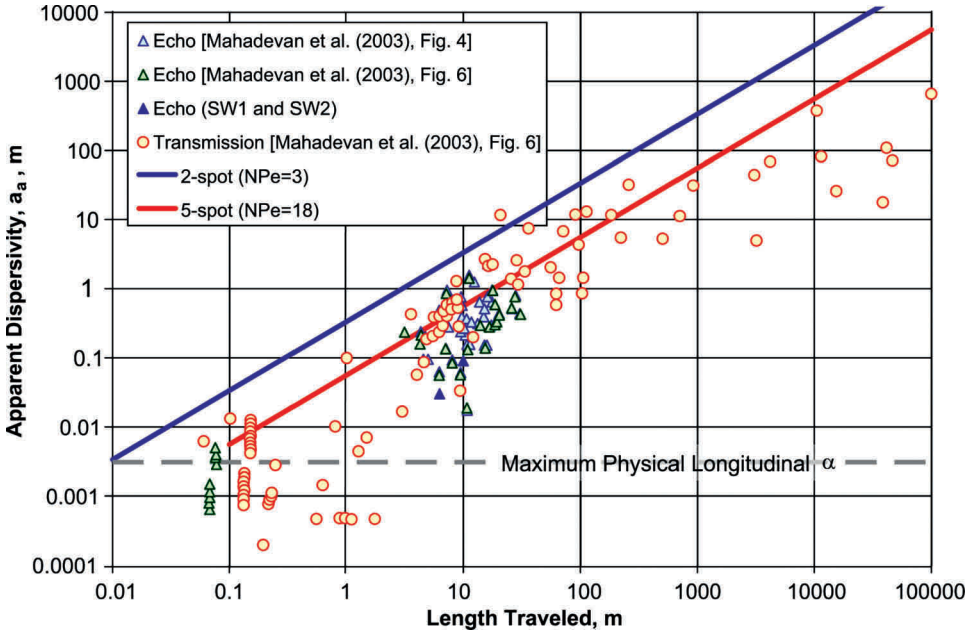

Fig. 4—Apparent dispersivity scale dependence with length traveled. Reported literature best fit CD data (symbols) and expected linear trend for constant N_{Pe} values in 1D CD Eq. 3, representing areal conformance (only) for two spot and five spot.

dispersivities to match field data affected by other conformance issues such as stratification and drift.

Stratification. Now we consider the case of stratification only (100% areal conformance), by use of various $k(z)$. For a given $k(z)$, the Muskat equation (Eq. 12) gives a unique $C(Q_D)$, by use of the step function for $F(Q_D)$. For example, by use of the log-normal $k(z)$ (Muskat 1949) and V=0.5 we obtain the result in **Fig. 5.** A fit of this profile to the C/D equation (Eq. 3) (for $0<Q_D<4$) gives an excellent best-fit apparent Peclet number of $N_{Pea}=N_{Peas}=3.5$. This corresponds to a scale-dependent apparent dispersivity for V=0.5:

$$\alpha_a = \frac{1}{3.5}L = 0.286L$$

Fig. 6 shows the α_a-vs.-L relationship for a number of values for three apparent Peclet numbers: 5, 50, and 500, superimposed on literature-reported α_a for a wide range of single- and two-well test data. This range of N_{Pea} brackets practically all the reported apparent dispersivities from field-test data. **Fig. 7** shows a plot of N_{Pea} vs. V (red line). An approximate relation for $N_{Pea}(V)$ was suggested by Warren and Skiba (Warren and Skiba 1964):

$$N_{Pea} \approx 2/[\ln(1-V)]^2, \quad \ldots\ldots\ldots\ldots\ldots\ldots\ldots\ldots\ldots\ldots \quad (15)$$

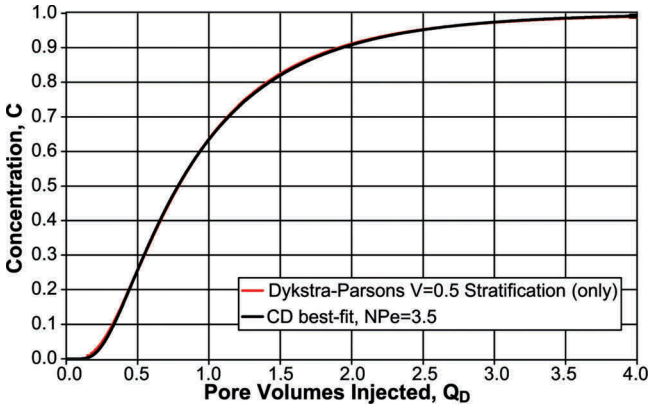

Fig. 5—Best-fit CD match of N_{Pe}=3.5 to log-normal Dykstra-Parsons V=0.5 stratification (red line); 100% areal conformance assumed.

which is accurate for $V<0.4$, but increasingly overpredicts N_{Pea} at $V>0.4$ (e.g., estimated $N_{Pea}=0.77$ at $V=0.8$ vs. the "correct" C/D best-fit value of $N_{Pea}=0.3$).

A similar analysis was performed for the Muskat linear and exponential $k(z)$ stratification. Results are shown in Fig. 7 (blue and pink lines, respectively).

For further discussion of the black circles and line on Fig. 7, see the Additive Conformance Dispersivities subsection at the end of Appendix A.

Stratified Five Spot. Let us consider the case of a stratified five-spot system. The Muskat solution (Eq. 12) is used to calculate $C(Q_D)$, by use of $F(Q_D)$ given by the five-spot solution (Eq. 7) and the log-normal $k(z)$ with V=0.353. **Fig. 8** shows $C(Q_D)$ and a near-exact C/D-equation (Eq. 3) best fit with apparent Peclet number N_{Pea}=6.

Best-fit N_{Peas}=10 for V=0.353 stratification alone. Best-fit N_{Peap}=18 for a five-spot pattern alone. By use of additive dispersivities (see Appendix), this five-spot stratified system has an effective Peclet number $N_{Pea} \approx 1/(1/18+1/10)=6.4$, close to the best-fit value of 6.

The Linearity of α_a-Scale Dependence. Muskat showed any well patterns (e.g., five spots or two spots) of different scales, L, with the same stratification in the absence of drift have the same effluent profile $C(Q_D)$ and the same best-fit Peclet number L/α_a. (Same stratification means the same value of $r=k_{max}/k_{min}$ or V for the three Muskat $k(z)$ models or for other $k(z)$, the same $k(z_D)$, remembering that the order of k is irrelevant.) The apparent dispersivities will plot exactly as a straight line of slope 1 on a log-log plot of α_a vs. L, with the intercept determined by its apparent Peclet number.

The Scatter of α_a-Scale Dependence. In general, if two systems have different stratifications or different well patterns (e.g., five spot vs. two spot), then they will have different Peclet numbers [different $C(Q_D)$ profile(s)]. This will clearly give rise to scatter in plots of α_a vs. L. This is complicated by the fact that systems with different stratifications may have the same Peclet number. As an example, three reservoirs with different stratification $k(z)$ descriptions were chosen: V=0.353, linear r=5.49, and exponential r=3.95. Areal conformance is taken as 100%. The $C(Q_D)$ solutions from the Muskat equation (Eq. 12) solution for each reservoir are shown as solid lines in **Fig. 9.** Slight differences in

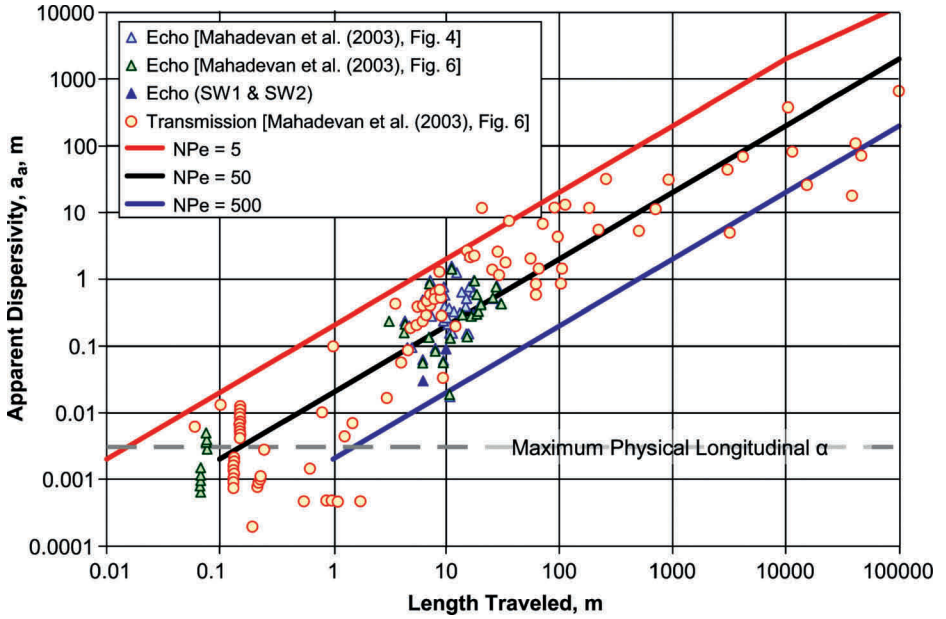

Fig. 6—Apparent dispersivity scale dependence with length traveled. Reported literature best-fit CD data (symbols) and expected linear trend for constant N_{Pe} values in 1D CD Eq. 3.

profiles are seen for the different stratifications, but each one is described by the same best-fit apparent Peclet number of 10 by use of the 1D C/D equation.

A System Without α_a-Scale Dependence. Consider an echo test with drift. The α_a-scale dependence becomes complicated if not void of meaning. The distance traveled, L, is $2L_m$, where $L_m^2 = Q_{inj}/\pi H\phi$. But $Q_{inj} = qt$ for a constant injection rate, which gives an infinite number of combinations of q and t (time at the end of injection) with the same Q_{inj} and therefore with the same L. For a fixed L, however, every valid combination of q and t results in a different $C(Q_D)$ relation with different apparent dispersivities. Obviously, this will lead to scatter, potentially severe, as shown in a later example. Furthermore, if two tests are run, each with a different L, the resulting apparent dispersivity can have any slope on a log-log plot of α_a vs. L: 0, ∞, -1, or (fortuitously) 1.

The problems just described are illustrated, on the basis of 3D sensor simulations made of the Pickens-Grisak single-well test area. After matching the two SW1 and SW2 echo tests with a model correctly describing the field-observed drift, a number

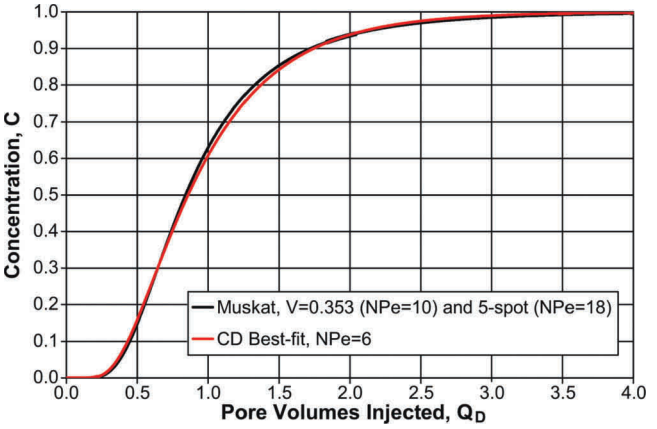

Fig. 8—Muskat solution to five-spot (N_{Pea}=18) with Dykstra-Parsons V=0.353 stratification (N_{Pea}=10), having CD best fit N_{Pea}=6.

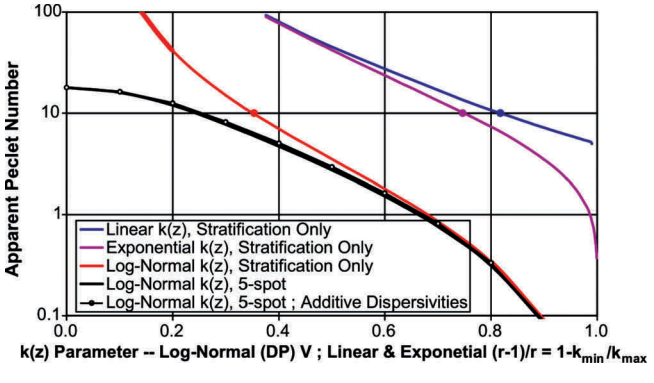

Fig. 7—Apparent Peclet number relation to stratification parameters (100% areal conformance assumed): log-normal Dykstra-Parsons V (red line); Muskat linear and exponential models (r–1)/r=1–k_{min}/k_{max} (blue and pink lines). Also shown is the composite five-spot areal with log-normal stratification (black line) conformance, with additive dispersivity approximation (black circles).

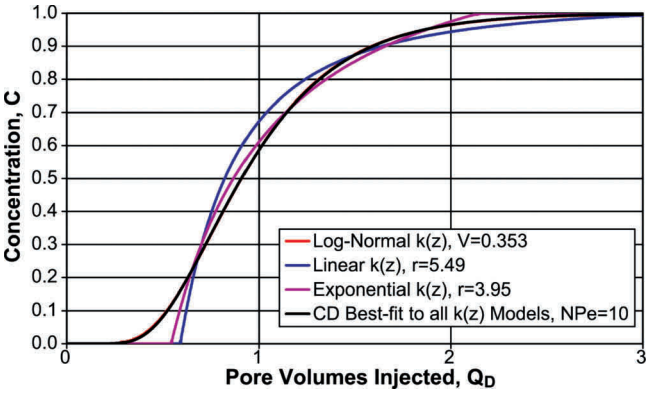

Fig. 9—Best-fit CD match of N_{Pe}=10 to three stratification $C(Q_D)$ relations (100% conformance assumed): log-normal Dykstra-Parsons V (red line); Muskat linear and exponential models (blue and pink lines). Best-fit CD and V=0.353 log-normal curves are coincident (near-perfect fit).

TABLE 1—SENSOR RADIAL MODEL WITH DRIFT—SIMULATION RESULTS FOR ECHO TESTS WITH VARYING RATE AND INJECTION PERIOD

		SW1 Rate			Half SW1 Rate	
L m	t_{inj} (days)	α_a m	N_{Pea}	t_{inj} (days)	α_a m	N_{Pea}
5.6	1	0.018	315.6	2	0.052	106.9
9.7	3	0.061	158.6	6	0.228	42.6
11.9	4.5	0.108	109.9	9	0.452	26.3
13.7	6	0.163	84.2	12	0.570	24.0
15.8	8	0.245	64.6	16	0.809	19.5

TABLE 2—GREENKORN ET AL. (1965) LAYER PROPERTIES FOR LABORATORY STRATIFIED FIVE-SPOT MODEL

Layer	h (ft)	k (darcies)
1	1.8	6.75
2	3.2	9.16
3	1.7	8.23

of echo-test simulations were made at two rates with varying injection periods. **Table 1** gives results of the simulated tests with best-fit apparent dispersivities for each test. If we randomly choose any two of the tests to define the system-scale dependence, the resulting slope on a log-log plot of α_a vs. L will range from 0 to $\pm\infty$. Halving the rate and doubling the injection period to maintain a constant L results in an apparent-dispersivity increase by a factor of 3 to 4 (i.e., severe "scatter"). For a fixed injection rate and varying injection period, the slope is approximately 2 but varies somewhat. See the SW1 and SW2 Echo Tests Including Drift, in the following subsection for further discussion.

Field and Laboratory Examples

Greenkorn Field and Scaled Laboratory Five Spots. This example supports our contentions that the large apparent dispersivities, α_a, of two-well field pilot tests reflect conformance and do not indicate or imply physical-dispersivity values significantly larger than laboratory-measured values; those large α_a are essentially fitting factors that force a false model containing large second-order dispersion terms to match observed results reflecting first-order conformance effects; and applying a correct model containing correct (low or laboratory) dispersivity can yield results matching observed results [i.e., the model dispersivity required to force a match between model and observed results will be the laboratory value (essentially 0, compared with the large reported apparent dispersivities)].

Greenkorn et al. (1965) conducted confined five-spot miscible-flood field tests for mobility ratios of 1, 0.1 (both favorable), and 10 (unfavorable). We discuss here only their unit-mobility results. They constructed a $22.3\times22.3\times6.7$-in quarter-five-spot laboratory model, scaled by a factor of 13.33 from their $50\times50\times8.4$-ft field (full) five-spot pilot. They used extensive field core-plug permeability data to replicate the field heterogeneity in a scaled manner in the laboratory model; permeability varied significantly with x, y, and z. The result was essentially exact agreement between the field-observed and scaled laboratory-model tracer-recovery curves [Fig. 8 in Greenkorn et al. (1965)].

They repacked their laboratory model with a less accurate heterogeneity: the three-layered, $k(z)$, description given in **Table 2.** The resulting laboratory-model tracer-recovery curve differed significantly from that of the field and the previously mentioned laboratory model with 3D "accurate" heterogeneity [Figs. 5 and 7 in Greenkorn et al. (1965)]. **Fig. 10** compares their layered laboratory-model recovery curve with the recovery curve we calculated from the Muskat equation (Eq. 12) by use of the five-spot analytical $F=C(Q_D)$ relation (Eq. 7) and layer properties in Table 2. The close agreement indicates that areal and vertical conformance dominate the effluent profile, while physical-dispersion effects in the laboratory model were negligible in comparison. The layered laboratory-model recovery curve may be accepted as the field-observed recovery curve if the field heterogeneity were the layering {on a scaled basis [i.e., same $k(z_D)$]} of the repacked layered laboratory model (Table 2).

We calculated an apparent Peclet number L/α_a of 16.25 from the best fit of Eq. 3 to the $C(Q_D)$ result from the Muskat-model solution as shown in **Fig. 11.** This $C(Q_D)$ solution and its Peclet number are scale-independent. The corresponding apparent dispersivity is $\alpha_a=0.0615L$, or 0.665 m for a layered field test by use of L=interwell distance=10.8 m, and assuming equivalent field and laboratory model descriptions. The apparent dispersivity from the laboratory model is 13.33 times less or 0.05 m. The field-scale apparent dispersivity of 0.665 m at a scale L of 10.8 m can be noted on Fig. 6 and agrees well with the conformance related

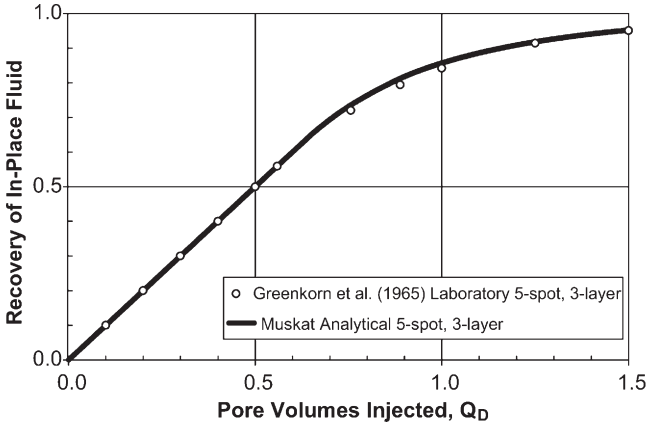

Fig. 10—Prediction of recovery performance of a laboratory five-spot, three-layer tracer test (Greenkorn et al. 1965) by use of the Muskat Eq. 12 analytical solution for a five-spot pattern and lab layer properties.

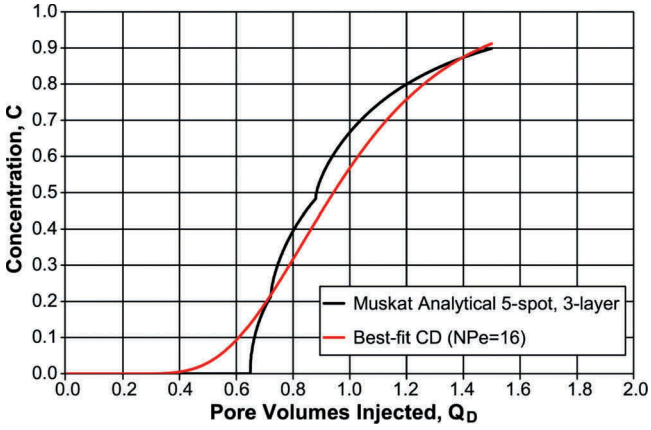

Fig. 11—CD best fit of the Muskat Eq. 12 analytical solution for a five-spot pattern and lab layer properties describing the Greenkorn (1965) laboratory test.

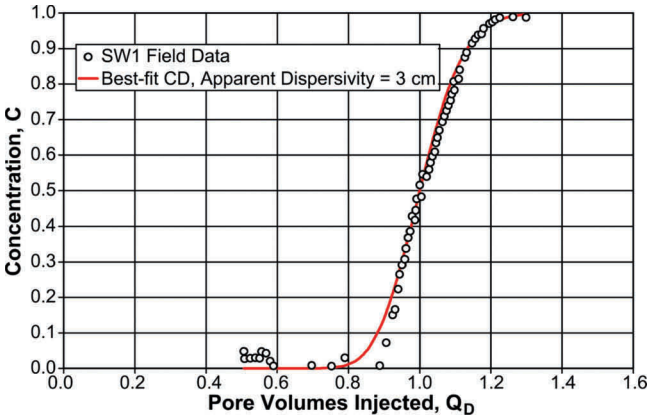

Fig. 12—Pickens-Grisak SW1 test data and best-fit CD model with N_{Pea}=209, α_a=3 cm.

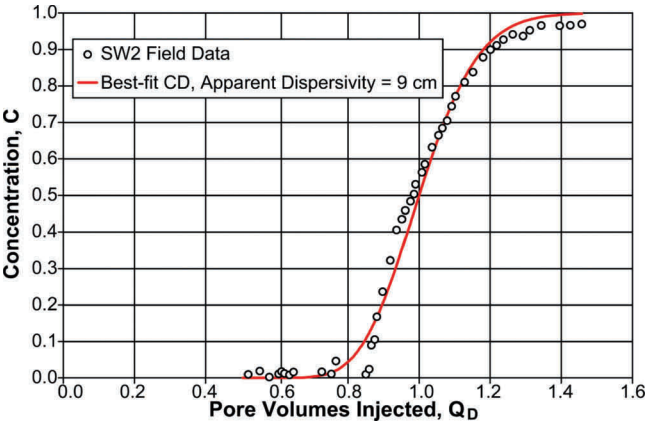

Fig. 13—Pickens-Grisak SW2 test data and best-fit CD model with N_{Pea}=118, α_a=9 cm.

field data points. Note that in this example: the 0.665 m apparent dispersivity is more than 200 times larger than a laboratory-measured dispersivity of ≈0.01 ft; the Muskat analytical solution closely matching the laboratory test data (Fig. 10) has no in-situ mixing, no dispersion, and no numerical dispersion; and the model dispersivity required for agreement between observed and "correct" model results is zero.

Pickens-Grisak (1981) Echo Tests. The single-well echo tests presented by Pickens and Grisak in 1981 are studied below. These authors provide detailed information about a groundwater system and two echo tests conducted in a single well. They fit the production profiles to a radial 1D C/D equation essentially equivalent to the simplified one-term linear 1D C/D equation (Eq. 4).

SW1 Echo Test. Apparent dispersivity of α_a=3 cm was reported for SW1. Travel distance was $L=2L_m$=6.26 m. Results are given in terms of a Q_p/Q_{inj} ratio which is related to Q_D by $Q_p/Q_{inj}=1+2(Q_D-1)$, or $Q_D=0.5(Q_p/Q_{inj}+1)$. Our fit of their observed profile to the linear C/D equation (Eq. 3) gives the same α_a=3 cm as shown in **Fig. 12.**

Pickens and Grisak do not give a quantitative model to explain an apparent dispersivity some 85 times their laboratory-measured physical dispersivity of 0.035 cm (0.00115 ft).

SW2 Echo Test. Apparent dispersivity of α_a=9 cm was reported for SW2. Travel distance was $L=2L_m$=10 m. Our fit of their observed profile to the linear C/D equation (Eq. 3) gives basically the same α_a=8.5 cm, as shown in **Fig. 13.**

Pickens and Grisak do not give a quantitative model to explain an apparent dispersivity some 250 times their laboratory-measured physical dispersivity of 0.035 cm (0.00115 ft).

SW1 and SW2 Echo Tests Including Drift. Pickens and Grisak state "the effect of natural regional flow is generally assumed to be negligible in the vicinity of the two wells" (one of the wells being the one used in SW1 and SW2). But the authors do provide detailed field data quantifying the regional groundwater-flow gradient (drift). Our interpretation of their Fig. 2 gives 0.0023 psi/ft at the location of the single- and two-well tests **(Fig. 14).**

We conducted a numerical model study with Sensor by use of an $r-\theta$ simulation of a single layer with 2,810-ft diameter and the test well at its center. Data were taken from the Pickens and Grisak SW2 test. Porosity was 0.38, permeability was 14.8 darcies (from their Eq. 24). The test-well injection and production rates were 14.5 and 12.22 RB/D/ft of thickness. Injection and production times were 3.93 and 9.326 days, respectively.

A 1,000 × 25 $r-\theta$ grid was used to represent the symmetrical half circle. The radial spacing was 999 equal-volume blocks from $r=r_w$=0.17 ft to r=20 ft and one block from r=20 to r=1,405 ft. Angular spacing was uniform with Δ=7.2°. Injection and production wells in cells (1,000, 25) and (1,000, 1), respectively, operated on pressure constraint to give a nearly uniform linear velocity gradient of ≈0.0023 psi/ft within the 40-ft diameter of the test-well region.

We made various simulations to evaluate numerical dispersion. For a zero hydraulic gradient, the radial spacing combined with running at the stable step (CFL=1) gave zero numerical dispersion, as shown by the step function on **Fig. 15.** Including the hydraulic gradient, numerical dispersion has a negligible effect on the calculated effluent curve because grids of 500 × 25 and 1,000 × 50 gave identical results (Fig. 15).

The resulting model comparison with test data is shown in Fig. 15 with what we consider to be an excellent match. Recall that the simulation results are based solely on a geological layer

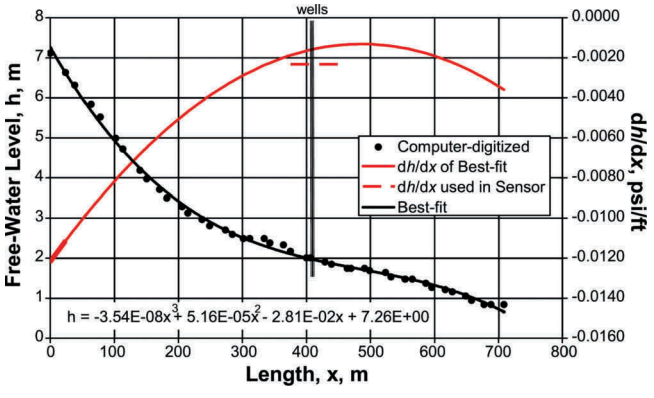

Fig. 14—Pickens-Grisak well test data for estimating drift gradient used in SW1, SW2, and two-well modeling.

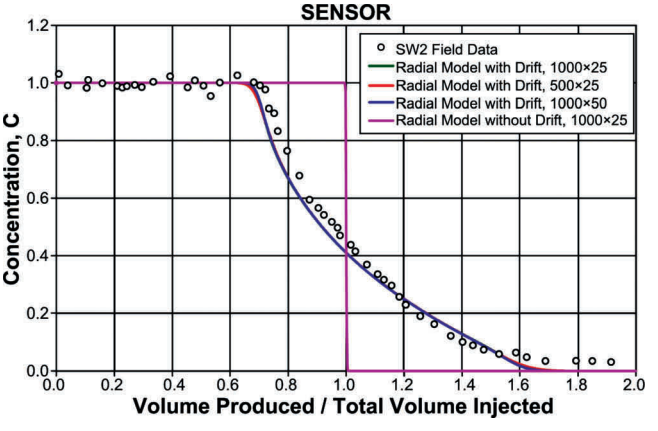

Fig. 15—Pickens-Grisak SW2 test data and SENSOR $r-\theta-z$ model with drift, and zero numerical dispersion (CFL=1).

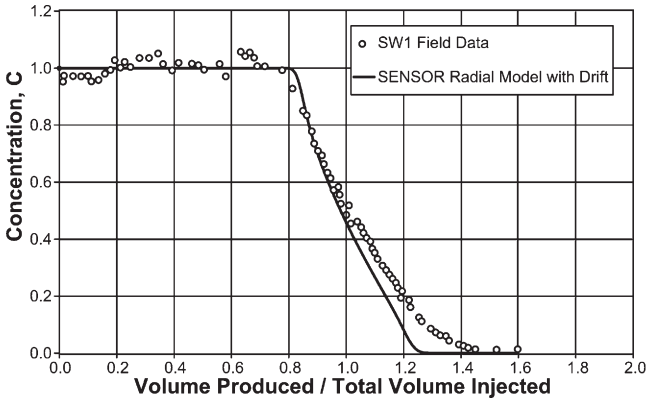

Fig. 16—Pickens-Grisak SW1 test data and Sensor *r*–*θ*–*z* model with drift.

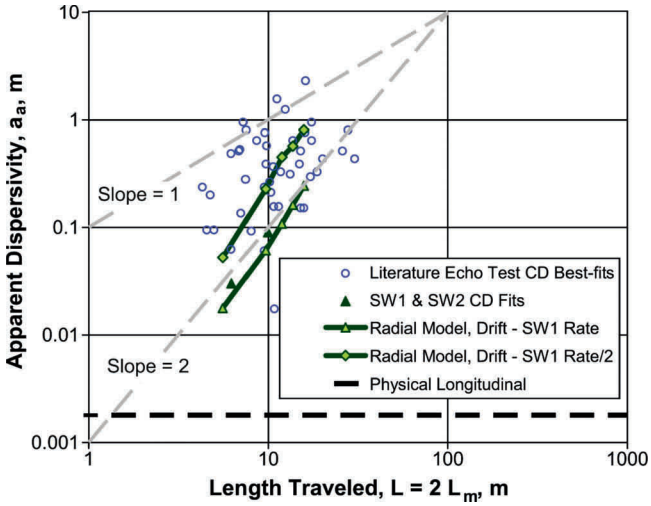

Fig. 17—Apparent dispersivity scale dependence for echo tests. Literature data (symbols) and Sensor simulated trends for Pickens-Grisak SW area wells with drift using two injection=production rates with varying injection periods.

description including measured drift (i.e., predictive and with no physical dispersion).

Fitting the model results with the C/D equation, we get a best-fit apparent dispersivity of 11 cm, close to to the 9 cm found when fitting the data themselves.

We also simulated the SW1 test with drift. The finely gridded well-test area was a circle 23 ft in diameter. Injection and production rates were 17.868 RB/D/ft. Injection and production times were 1.25 and 2 days, respectively. **Fig. 16** compares observed and calculated results (for $1{,}000\times25$ grid) of effluent profiles with a good match.

The best-fit apparent dispersivity to our model profile is 1.6 cm compared with 3 cm when fit to the data directly.

We repeated the above SENSOR r–θ runs with r–θ–z runs by use of the layered $k(z)$ description tabulated by Pickens and Grisak. These runs showed very little effect of the stratification.

With a predictive model to describe the well used for SW1 and SW2 tests, we ran a number of simulations to study the relation of apparent dispersivity to travel distance ($2L_m$). A constant-rate test was simulated for varying injection periods: 1-, 3-, 4.5-, 6-, and 8-day runs for each rate. The first rate was the same as used in SW1, 17.868 RB/D/ft, and the second series of simulations used a rate one-half that value. Results are shown in Table 1 and **Fig. 17,** and they are discussed in the previous section. **Fig. 18** illustrates how two echo tests with identical length scales of 9.7 m have dramatically different $C(Q_D)$ profiles because of drift.

SW2 Echo-Test Modeling With Lamination and Physical Transverse Dispersion. Pickens and Grisak note that transverse dispersion between layers may give apparent echo dispersivity larger than physical dispersivity. They reported laminations 0.1 to 0.5 cm thick, textural variations over several to tens of cm, and an 18-layer (each 45 cm thick) $k(z)$ description, but they gave no estimate of adjacent-sublayer or -lamination permeability contrasts.

A SENSOR simulation of echo-test SW2 was built by use of a description of alternating layers of thickness, h, with a permeability ratio of 3:1 with no drift. The symmetrical element is two adjacent layers, each of thickness $h/2$. The 2D r–z C/D equation was solved with longitudinal $K_\ell=0$ and $K_t=D^*+\alpha_t u(z)$ by use of a computational r–z grid of $1{,}000\times8$. The radial spacing corresponded to equal-volume gridblocks between $r=r_w=0.17$ ft and outer radius $r_e=22$ ft. This spacing and use of the maximum stable step minimized numerical dispersion. Numerical dispersion was determined from a run with $K_t=0$. The SW2 rate of 14.5 RB/D/ft and injection time of 3.93 days were used. Effective molecular diffusion, D^*, was 0.001 ft^2/day corresponding to a liquid/liquid molecular-diffusion coefficient of approximately $2\cdot10^{-5}$ cm^2/s and a tortuosity of 2. Transverse dispersivity was 0.0035 cm (10 times less than the laboratory-measured α of 0.035 cm).

Fig. 19 compares observed and model C vs. Q_p/Q_{inj} for layer thickness=0.08 ft (2.44 cm). The best-fit apparent dispersivity, α_a, for the model effluent curve is 11 cm. We estimate that numerical dispersion contributed <2% of that value. The simulation used withdrawal rate equal to injection rate, whereas the test withdrawal rate was actually somewhat less than injection rate. The description used is simplistic relative to the many possible

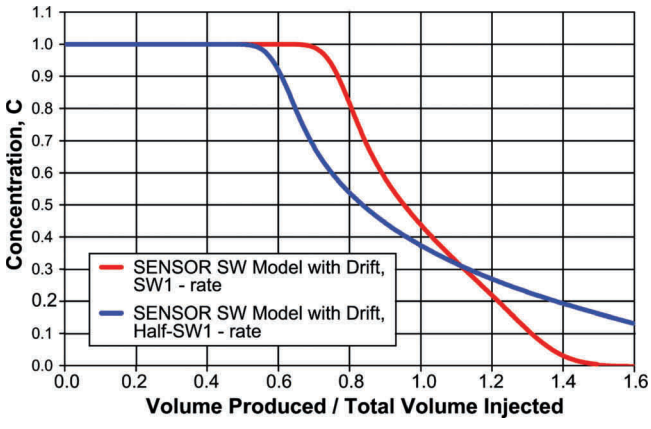

Fig. 18—Pickens-Grisak SW test area, Sensor model predictions with drift for two injection-production rates; L_m=9.7 m (three days at SW1-rate, six days at half SW1 rate).

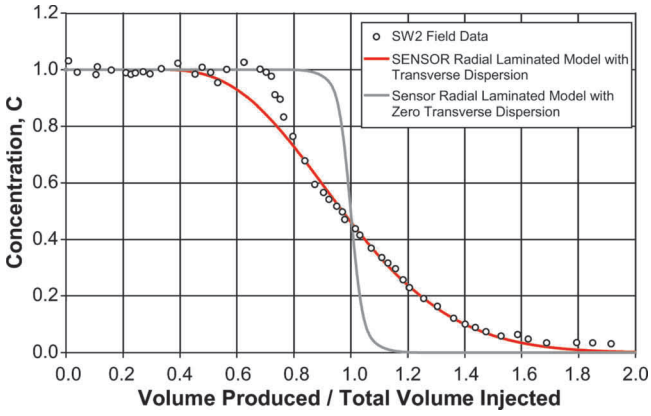

Fig. 19—Pickens-Grisak SW2 test data and Sensor *r*–*θ*–*z* model with thin laminations (2.44 cm) with 3:1 *k*-contrast, α_t=0.0035 cm, $D_0=2\cdot10^{-5}$ cm^2/s, no drift, and only minor (<2%) numerical dispersion.

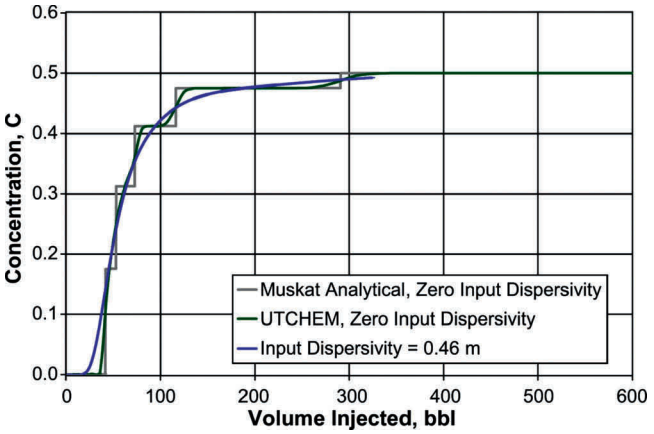

Fig. 20—Pickens-Grisak two-well transmission test results with recycling of produced tracer. Comparison of SENSOR *r–θ–z* model with measured stratification and drift for re-injection of model-produced water (red line) and injecting field-measured concentrations (black line); also, single-layer two-spot solution without drift and by use of apparent dispersivity [Grove model (Pickens and Grisak 1981)].

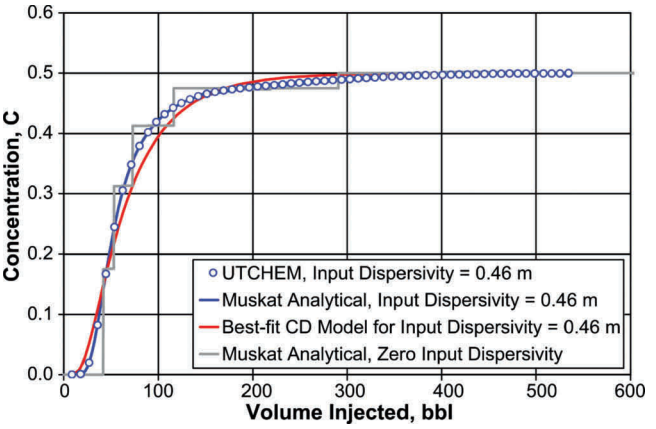

Fig. 21—Mahadevan et al. (2002) five-layer *x-z* cross-sectional transmission test with input dispersivity 0.46 m, comparing UTCHEM numerical solution (blue circles) with Muskat Eq. 12 analytical model (blue line). Zero-dispersion solution (gray line). Best-fit CD model for input =0.46 m is N_{Pe}=2.24 (red line).

variable permutations and depth-dependent variations in those permutations; the results nevertheless indicate transverse dispersion can give apparent echo dispersivities two to three orders of magnitude larger than laboratory-measured values. Note that there is no crossflow in this problem (i.e., vertical permeability is irrelevant).

We have stated earlier that heterogeneity alone causes no in-situ mixing. Here, there is in-situ mixing and heterogeneity. But this mixing is caused by flow with transverse dispersivity $\alpha_t>0$. The level of heterogeneity affects the amount of mixing caused by flow with $\alpha_t>0$, but the heterogeneity does not *cause* the mixing. Heterogeneity alone ($\alpha=\alpha_t=D_0=0$) causes no in-situ mixing. If α_t were 0 in the heterogeneous case of this subsection, there would be no in-situ mixing.

Pickens and Grisak (1981) Two-Well Test. This is a 15-day recirculating two-well tracer test with an interwell distance of 8 m reported by Pickens and Grisak (1981). **Fig. 20** [Fig. 14 in Pickens and Grisak (1981)] compares their observed effluent profile with the calculated profile from a single-layer two-spot numerical model proposed by Grove (Pickens and Grisak 1981) with an apparent dispersivity α_a=50 cm.

A SENSOR run was made by use of a $1{,}000\times25\times6$ $r-\theta-z$ (i,j,k) grid with the producer at the center for the symmetrical half circle. The grid used 999 equal-volume radial gridblocks between $r=r_w$=0.17 ft and r=40 ft, r_e=1,405 ft, and uniform angular spacing Δ=7.2°. Injection and production wells at (1,000, 25) and (1,000, 1), respectively, were operated on pressure constraint to give a nearly uniform linear drift gradient of 0.0023 psi/ft in the 80-ft-diameter test area. The test injection well was positioned at j=25, 8 m upstream (relative to drift) from the producer. All wells were completed in all six layers. Numerical dispersion was found to be very low by comparing a single-layer SENSOR run with no drift to the analytical two-spot solution (Eq. 8). The six-layer description used is a good approximation to the 18-layer description tabulated by Pickens and Grisak (1981).

The first SENSOR run used injected concentration equal to internally calculated produced concentration after 3.22 days, representing recirculation. Fig. 20 shows the SENSOR results (red curve).

Fig. 20 also shows measured concentrations for the production well (gray circles) and for the injection well (black circles) (Pickens et al. 1980) We have no explanation for the difference between concentrations measured from the same stream at the production well and the injection well other than data uncertainty.

A second SENSOR run was made by use of the reported injection concentration profile for $t>3.22$ days (black circles in Fig. 20), resulting in the calculated effluent profile shown in Fig. 20 (black line).

Both SENSOR predictions, on the basis of field-measured reservoir description (stratification and drift), predict effluent profiles consistent with measured breakthrough time of 3 days, time of maximum concentration ≈7 days, maximum concentration 0.21 to 0.27, and "flattening" concentration level of ≈0.2 for $t>10$ days. Given that this same reservoir description, with zero input physical dispersion, also predicts accurately the SW1 and SW2 single-well tests at the same well location, we suggest that the test-area conformance is adequately history matched by modeling stratification and drift only without the need for apparent dispersivity.

Areal heterogeneity and/or different layered descriptions were not explored. These factors could possibly help to fine tune the history match.

Modeling Examples

Mahadevan et al. (2003). This paper presents a number of simulation studies conducted to provide understanding of apparent dispersivities. We discuss several issues brought forth in that paper, and a somewhat different interpretation of results is presented therein.

Five-Layer Problem. Their example is a 30 × 20-ft layered x–z cross section used to numerically simulate a two-well field tracer test by use of a 30 × 5 x–z grid. Layer permeabilities are 200, 500, 800, 1,100, and 1,400 md, each 4 ft thick. One pore volume is 72.66 RB. They used large input dispersivities of α=0.46 m and α_t =0.046 m [α_t has no effect.* Crossflow does not exist, so vertical permeability is irrelevant.

The analytical solution for the transmission effluent curve is given by Muskat's equation (Eq. 12) by use of the base function F from Eq. 3. **Fig. 21** shows the Muskat analytical solutions for input α=0 and for input α=0.46 m. The Mahadevan et al. (2003) simulated effluent profile (for input α=0.46 m) is in exact agreement with the Muskat solution shown in Fig. 21.

The Muskat effluent profiles yield best-fit apparent dispersivities of 1.63 m and 2.24 m for α=0 and α=0.46 m, respectively. This α_a=2.24 m is roughly equal to the sum of conformance and input ("physical") dispersivities, $\alpha_a=\alpha_{ac}+\alpha$ (=1.63+0.46), which is the additive dispersivity equation (Eq. A-1).

For input α of zero, the Muskat analytical solution gives α_a= 1.63 m and reflects no mixing in the reservoir. This large α_a reflects only conformance of the layer heterogeneity and is >500 times larger than a typical laboratory-measured physical $\alpha\approx0.01$ ft. **Fig. 22** shows the accuracy of the UTCHEM solution for input α=0, compared with the Muskat analytical solution.

*Personal communication with J. Mahavedan. January 2004.

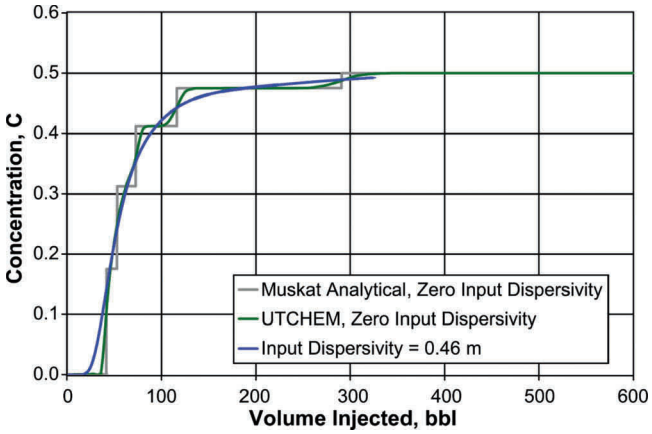

Fig. 22—Mahadevan et al. (2002) five-layer *x-z* cross-sectional transmission test with zero-input dispersivity, comparing analytical Muskat solution (gray line) with UTCHEM higher-order difference scheme (green line); solution with input dispersivity 0.46 m also shown (blue line).

The Muskat C profile for α=0 and its best-fit Peclet number ($N_{Pe\alpha}=L/\alpha_a$=5.61) are scale-independent (independent of L and H). The scale dependence of α_a (=L/5.61) is a meaningless consequence of applying the nonapplicable C/D equation (Eq. 3) to a profile dominated by conformance.

Eight-Layer Problem, k_v=0. This problem is an x-z cross section with k_v=0, eight 2.5-ft-thick layers, and a stochastic permeability distribution. Mahadevan et al. (2003) numerically simulated this system to obtain apparent dispersivities for two-well (transmission) and single-well (echo) tracer tests. They used $N_x \times 8$ grids with a uniform cell size of 1×2.5 ft and large input dispersivities of α=0.46 m and α_t=0.046 m.

This problem is the same type of problem as the five-layer problem discussed above (i.e., a layered 2D x-z cross section with no crossflow). The permeability, k_j, of layer j is the harmonic average $k_j(L/\Delta x)/\sum_i k_{ij}^{-1}$, where the summation is from i=1 to N_x. SENSOR numerical solutions show negligible effects of transverse dispersion for α_t<0.0046 m, which is 15 times larger than a physical value ≈0.001 ft. Therefore, Muskat's equation (Eq. 12) gives the analytical solution to this problem for α_t<0.0046 m and any value of α. The analytical effluent profiles give the following transmission apparent dispersivities, α, (m):

	Apparent Dispersivities α_a (m) for Model	
Length L (ft)	Input α=0	Input α=0.46 m
30	11.4	12.1
60	31.4	32.4
100	56.4	57.6

The large apparent dispersivities reflect only conformance and provide no support for large physical dispersivities. The additive dispersivity relation (Eq. A-1) becomes more approximate as L and α_a increase.

Eight-Layer Problem, k_v=k_h. These simulations use k_v=k_h. for the same problem just described. Because crossflow exists the Muskat solution does not apply. Mahadevan et al. numerically simulated this problem to obtain apparent transmission, echo, and local dispersivities [Fig. 10 in Mahadevan et al. (2003)]. They used large input dispersivities α=0.46 m and α_t=0.046 m. Local dispersivities are those obtained from individual-gridblock $C(t)$ profiles.

Their reported local and echo dispersivities and scale dependence of the latter reflect significant numerical dispersion. A simple way to check numerical-dispersion levels is to perform simulations by use of zero input dispersivities. For the runs and results described here, we ran UTCHEM by use of their data sets. **Fig. 23** shows individual-cell $C(t)$ profiles for the transmission case L=60 ft by use of zero input dispersivities. The profiles differ significantly from expected zero-dispersivity vertical step functions from 0 to 1. Best-fit local apparent dispersivities (by use of L=i ft, Δx was 1 ft) for the profiles shown range from 0.042 to 0.952 m and reflect only numerical dispersion.

By use of zero input dispersivities, we ran UTCHEM echo tests for scale L=22.06, 44.12, and 80.88 ft. **Fig. 24** shows the C profile for L=80.88 ft. The profile for input α=α_t=0 shows significant numerical dispersion (the correct profile is a step function from 1.0 to 0 at Q_D=1.0). Arguably, the correct profile for α=0.46 m corresponds to Eq. 3 shown in Fig. 24. We believe numerical dispersion affects the apparent echo dispersivities (2 m at L=80.88 ft) and the scale dependence shown in the of Mahadevan et al. (2003) Fig. 10.

Discussion

No scale-dependent dispersivity entered into numerical simulation models can represent physical dispersion correctly. Many papers (Mahadevan et al. 2003; Solano et al. 2001; Stalkup 1998; Johns

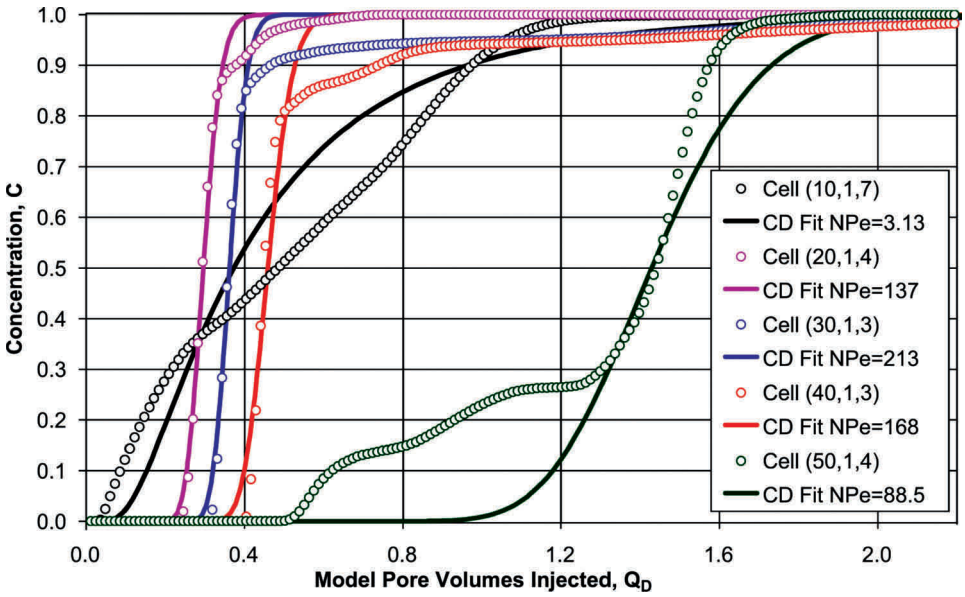

Fig. 23—Mahadevan et al. (2002) UTCHEM eight-layer *x-z* cross-sectional transmission test with zero-input dispersivity, showing individual-cell concentration profiles' variation during the test. Best-fit CD Eq. 3 lines also shown.

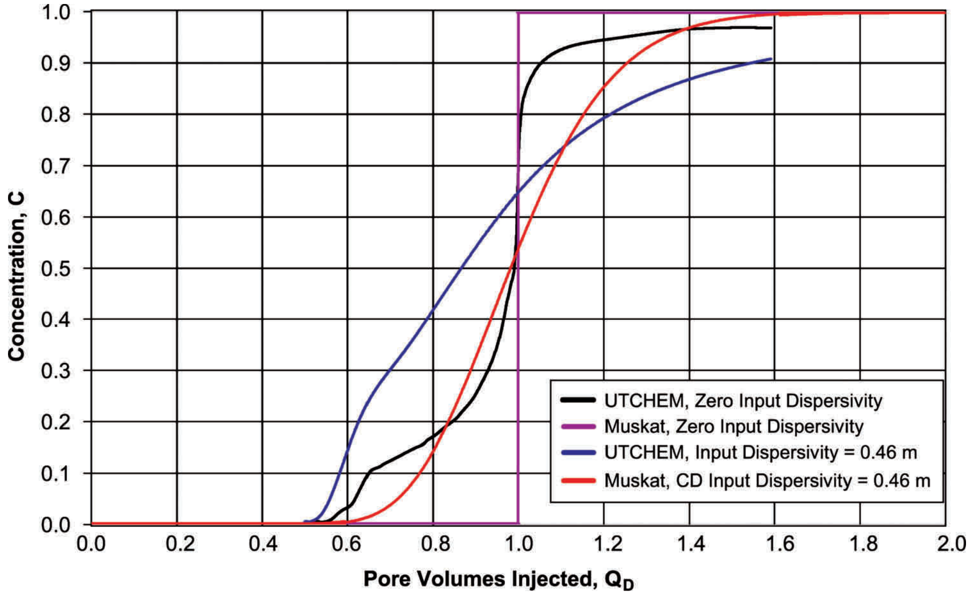

Fig. 24—Mahadevan et al. (2002) UTCHEM eight-layer *x–z* cross-sectional echo test for *L*=80.88 ft, illustrating numerical dispersion error (black and blue lines). Exact solutions are given by Muskat model (pink and red lines).

et al. 2000; Moulds et al. 2005; Kelkar and Gupta 1988) present numerical simulations by use of a scale-dependent input dispersivity to represent effects of physical dispersion on first-contact miscibility (FCM) and multiple-contact miscibility (MCM) for continuous or bank injection of tracer, solvent, or enriched gas. Their conclusions that their results reflect or approximate effects of physical dispersion are highly questionable. By use of a large scale-dependent input dispersivity α_a, they fail to distinguish between dispersion and conformance. Examples of this include the statement: "Dispersion is a measure of the extent to whichfluids become irreversibly mixed at the molecular scale" (Moulds et al. 2005). We accept this as a definition of physical dispersion. Another statement, "Classical theory shows that dispersion scales with distance" (Moulds et al. 2005), relates to conformance.

We illustrate the preceding statement by use of the paper by Moulds et al. (2005). They note a laboratory (say 1 ft) slimtube dispersivity of α=.02 ft and an L=100 ft echo-test dispersivity of 2 ft give Peclet numbers of 50. They say Peclet number is the appropriate measure to compare systems of different length from laboratory slimtube to reservoir cross sections. They then use P_e= 50 in a 1D MCM simulation to predict the effect of dispersion on oil saturations and compositions in a Prudhoe Bay observation (cored) well positioned 1,500 ft from the nearest enriched-gas injector. The P_e=50 of that simulation gives an input scale-dependent dispersivity α_a (L/P_e) of 30 ft, some 1,500 times larger than laboratory dispersivity. They assume P_e to be invariant with scale, L, meaning that dispersivity increases linearly with scale (L or distance traveled). Use of this scale-dependent α_a=30 ft in their 1D numerical solution of the C/D equation cannot represent physical dispersion. If dispersivity increases linearly with length (distance traveled) and a simulator input value of α_a=30 ft is used to generate results at 1,500 ft, then a value of α_a=2 ft is required to represent the level of "mixing" at x=100 ft. The input α_a=30 ft is 15 times too large to represent the amount of "mixing" at x=100 ft. If the simulator input α_a were 2 ft, results would arguably model the "mixing" at x=100 ft, but that α_a would be 15 times too small to model the "mixing" at 1,500 ft correctly. To put this in other words, if they had two cored observation wells, one at x=100 ft and, the other at x=1,500 ft from the injector, what α [or $\alpha(x)$] would they entered into their 1D simulator to explain or match the cored saturation/composition data from both wells? Any scale-dependent dispersivity input to a numerical model (used in the second-order Fickian term of type $K\partial^2C/\partial x^2$, $K=\alpha u$) is simply a fitting factor capable of approximating only the effluent profile of a single production well at a single fixed distance from the injector. Here, we have used the term "mixing" (at x) to denote the mixed-zone length between C=0.1 and C=0.9 at time $t=x/u$.

Our paper in part presents in detail a history match of one of the most thoroughly documented published field tracer tests (Pickens and Grisak 1981). That paper dismissed the influence of drift, which they stated is present in their field data, and found an α_a of 50 cm (1,428 times larger than the laboratory-measured 0.035 cm) necessary to match the effluent profile. We found a good match by use of drift alone, with zero dispersivity.

In relation to that field test, our paper addresses a published field tracer test of similar type (Greenkorn et al. 1965), where the long-used conventional petroleum-engineering approach of defining the heterogeneity (from core plugs) gave a close match of the effluent profile by use of zero dispersivity. The observed field test effluent profile was matched by its model in each case (Pickens and Grisak 1981; Greenkorn et al. 1965). But one model (Pickens and Grisak 1981) used a large scale-dependent dispersivity, while the other (Greenkorn et al. 1965) captured conformities (heterogeneity) with zero dispersion in its model grid (which we recommend).

Papers, including this one, often imply that "lab" dispersivity and physical [rock (Kelkar and Gupta 1988)] dispersivity are the same quantities with the same values. The Appendix shows that an additive dispersivity principle,

$$\alpha_a = \alpha + \alpha_{ac}, \quad \text{(16)}$$

is quite accurate at any scale, from laboratory (core-plug or packed-column) scale to reservoir scale. The laboratory dispersivity is α_a. Is this laboratory α_a indeed equal to α? If not, how can the value of α be estimated or determined? The Appendix shows the answer to the first question is "not necessarily." Core plug α_a can be much larger than α. The answer to the second question is obvious with use of Eq. 16. Physical dispersivity, α, reflects microscale heterogeneity and is scale-independent, while α_{ac} reflects (macroscale) heterogeneity and is scale-dependent. Thus, if laboratory tests for different lengths (scales) of the same material give the same α_a, then α_a=a. But there are few reports of such different-length laboratory tests. It is easier to compose and test different-length, same-material tests for packed columns than for cores. The α_a from different-length packed columns were found to be scale-independent (and therefore=α) by Blackwell (1962), Aronofsky and Heller (1957), and Brigham et al. (1961).

A consequence of this additive dispersivity principle is that physical dispersivity, α, is no larger than observed (apparent) laboratory test dispersivity α_a. Thus, the fact that very few reported laboratory dispersivities α_a exceed 1 cm (0.03 ft) supports the statements throughout this paper that physical dispersivity, α, is less than 1 cm.

Conclusions

1. Heterogeneity alone ($\alpha=\alpha_t=D_0=0$) causes no in-situ mixing in the reservoir.
2. Physical dispersivity, α, is a rock property on the order of 0.01 ft for consolidated rocks and significantly smaller for unconsolidated sand (bead) packs. It is independent of time and scale, regardless of whether scale is defined as system length, distance traveled, or "scale of heterogeneity."
3. Apparent dispersivity, α_a, is obtained by matching observed or numerically calculated effluent concentration curves with the 1D CD equation. That equation does not physically describe field-tracer-test behavior. That behavior largely reflects areal and vertical conformance, which in turn depend upon well pattern and completion intervals, heterogeneity, and drift.
4. The observed scale dependence of apparent dispersivity is void of meaning. When it exists, it is a necessary consequence of applying the nonapplicable 1D C/D equation with its single parameter, the Peclet number L/α, to match effluent profiles reflecting conformance.
5. A scale-dependent dispersivity cannot be used in numerical simulations to represent dispersion and its effects on FCM or MCM displacements, bank breakdown, and field tracer tests.
6. A scale-dependent dispersivity can be used only as a fitting factor to match or explain the effluent profile of a single producer at a fixed distance from an injector. It has no predictive value in any numerical simulation.
7. Numerical simulations designed to reflect the effects of physical dispersion on any reservoir displacement process should use scale-independent physical dispersivities on the order of 0.01 ft.

Nomenclature

b = parameter in Muskat exponential $k(z)$ equation, $=\ln(k_{max}/k_{min})$
C = concentration, fraction, normalized to 1.0 for initial injected-tracer concentration
D^* = effective molecular diffusion within a porous medium, cm^2/s [L^2/T]
D_0 = molecular-diffusion coefficient, cm^2/s [L^2/T]
f = =least-squares function
F = function $F(Q_D)$ describing the areal variation of concentration used in Muskat's analytical equation that composites areal and vertical conformance
h = layer thickness, ft or m [L]
H = total formation thickness, ft or m [L]
k = permeability, md [L^2]
k_{ij} = permeability in cell i,j, md [L^2]
k_j = permeability in layer j, md [L^2]
k_v = vertical permeability, md [L^2]
K = elliptic integral of first kind
K_ℓ = longitudinal dispersion coefficient, ft^2/s or cm^2/s [L^2/T]
K_t = transverse dispersion coefficient, ft^2/s or cm^2/s [L^2/T]
L = travel distance or length, ft or m [L]
L_m = mean depth of penetration in echo test, ft or m [L]
M = mobility ratio
N_{Pe} = Peclet number, dimensionless
N_{Pea} = apparent Peclet number, dimensionless
N_{Peac} = apparent Peclet number owing only to conformance, dimensionless
N_{Peap} = apparent Peclet number owing only to areal conformance, dimensionless
N_{Peas} = apparent Peclet number owing only to stratification (vertical) conformance, dimensionless
N_{PeL} = Peclet number in linear C/D equation, dimensionless
N_{PeR} = Peclet number in radial C/D equation (Gelhar and Collins 1971), dimensionless
q = volumetric rate (injection rate), B/D or m^3/d [L^3/T]
Q_D = pore volumes injected, dimensionless
Q_{DBT} = pore volumes injected at breakthrough, dimensionless
Q_{Dz} = pore volumes injected into a given layer z, dimensionless
Q_{inj} = total volume injected in an echo test, ft^3 or m^3 [L^3]
Q_p = volume produced in an echo test, ft^3 or m^3 [L^3]
r = parameter in Muskat $k(z)$ equations, $=k_{max}/k_{min}$
r_e = external-boundary radius, ft or m [L]
r_w = wellbore radius, ft or m [L]
t = time [T]
u = pore velocity, ft/d or m/d [L/T]
V = parameter in Dykstra-Parsons $k(z)$ log-normal distribution $=1-e^{-\sigma}$
w = width, ft or m [L]
x, y, z = Cartesian coordinates, ft or m (L)
x_D, y_D, z_D = dimensionless coordinates, x/L, y/w, z/H
z = vertical depth, ft or m [L]
α = physical (longitudinal) dispersivity, ft or m [L]
α_t = physical transverse dispersivity, ft or m [L]
α_a = apparent dispersivity, ft or m [L]
α_{ac} = apparent dispersivity owing only to conformance, ft or m [L]
α_{ap} = apparent dispersivity owing only to areal conformance, ft or m [L]
α_{as} = apparent dispersivity owing only to stratification $k(z)$ (areal conformance=100%), ft or m [L]
Δx = grid-cell length in x-direction (primary flow direction), ft or m [L]
θ = angle in a cylindrical coordinate system
σ = standard deviation in probability distribution
τ = tortuosity, dimensionless
ϕ = porosity, fraction
Ψ = $\ln(k/k_{min})$

Acknowledgments

The authors would like to thank Marco Thiele for helping prepare the contour map in Fig. 1, and Lee Chin and Ray Pierson for their assistance with the UTCHEM simulations.

References

Aronofsky, J.W. and Heller, J.P. 1957. Diffusion Model to Explain Mixing of Flowing Miscible Fluids in Porous Media. *Trans.,* AIME, **210:** 345–349. SPE-860-G.

Arya, A., Hewett, T.A., Larson, R.G., and Lake, L.W. 1988. Dispersion and Reservoir Heterogeneity. *SPERE* **3** (1): 139–148. SPE-14364-PA. DOI: 10.2118/14364-PA.

Blackwell, R.J. 1962. Laboratory Studies of Microscopic Dispersion Phenomena. *SPEJ* **2** (1), 1–8; *Trans.,* AIME, **225.** SPE-1483-G. DOI: 10.2118/1483-G.

Brigham, W.E., Reed, P.W., and Dew, J.N. 1961. Experiments on Mixing During Miscible Displacement in Porous Media. *SPEJ* **1** (1): 1–8; *Trans.,* AIME, **222.** SPE-1430-G. DOI: 10.2118/1430-G.

Dykstra, H. and Parsons, R.L. 1950. The prediction of oil recovery by waterflooding. In *Secondary Recovery of Oil in the United States*, second edition, 160–174. Washington, DC: API.

Gelhar, L.W. and Collins, M.A. 1971. General analysis of longitudinal dispersion in nonuniform flow. *Water Resources Research* **7** (6): 1511–1521. DOI:10.1029/WR007i006p01511.

Greenkorn, R.A., Johnson, C.R., and Harding, R.E. 1965. Miscible Displacement in a Controlled Natural System. *JPT* **17** (11): 1329–1335; *Trans.,* AIME, **234.** SPE-1232-PA. DOI: 10.2118/1232-PA.
Hagoort, J. 1982. The Response of Interwell Tracer Tests in Watered-Out Reservoirs. Paper SPE 11131 presented at the SPE Annual Technical Conference and Exhibition, New Orleans, 26–29 September. DOI: 10.2118/11131-MS.
Johns, R.T., Pashupati, S., and Subramanian, S.K. 2000. Effect of Gas Enrichment Above the MME on Oil Recovery in Enriched-Gas Floods. *SPEJ* **5** (3): 331–338. SPE-65704-PA. DOI: 10.2118/65704-PA.
Kelkar, B.G. and Gupta, S.P. 1988. The Effects of Small-Scale Heterogeneities on the Effective Dispersivity of Porous Medium. Paper SPE 17339 presented at the SPE Enhanced Oil Recovery Symposium, Tulsa, 16–21 April. DOI: 10.2118/17339-MS.
Kossack, C.A. 1989. The Dispersive Effect of Variable Layer Lengths on Miscible Displacements in Layered Heterogeneous Porous Media. *SPERE* **4** (2): 165–170; *Trans.,* AIME, **287.** SPE-17267-PA. DOI: 10.2118/17267-PA.
Mahadevan, J., Lake, L.W., and Johns, R.T. 2003. Estimation of True Dispersivity in Field-Scale Permeable Media. *SPEJ* **8** (3): 272–279. SPE-86303-PA. DOI: 10.2118/86303-PA.
Mercado, A. 1967. Spreading pattern of injected water in a permeability stratified aquifer. *Intl. Unio Geod. Geophys. Publ.* **72:** 23–36.
Morel-Seytoux, H.J. 1965. Analytical Numerical Method in Waterflooding Predictions. *SPEJ* **5** (3): 247–258; *Trans.,* AIME, **234.** SPE-985-PA. DOI: 10.2118/985-PA.
Moulds, T.P., McGuire, P.L., Jerauld, G.R., Lee, S.-T., and Solano, R. 2005. Pt. McIntyre: A Case Study of Gas Enrichment Above MME. *SPEREE* **8** (3): 182–188. SPE-84185-PA. DOI: 10.2118/84185-PA.Muskat, M. 1949. Effect of Permeability Stratification in Cycling Operations. *Trans.,* AIME, **179:** 313–328. SPE-949313-G.
Perkins, T.K., and Johnston, O.C. 1963. A Review of Diffusion and Dispersion in Porous Media. *SPEJ* **3** (1): 70–84; *Trans.,* AIME, **228.** SPE-480-PA. DOI: 10.2118/480-PA.
Pickens, J.F. and Grisak, G.E. 1981. Scale-dependent dispersion in a stratified granular aquifer. *Water Resources Research* **17** (4): 1191–1211.
Pickens, J.F., Merritt, W.F., and Cherry, J.A. 1980. Field determination of the physical contaminant transport parameters in a sandy aquifer. In *Nuclear Techniques in Water Pollution Research*, 239–265. Vienna, Austria: International Atomic Energy Agency.
SENSOR. 2004. Coats Engineering, Marco Island, Florida, www.coatsengineering.com.
Shrivastava, V.K., Nghiem, L.X., and Moore, R.G. 2002. A Novel Approach for Incorporating Physical Dispersion in Miscible Displacement. Paper SPE 77724 presented at the SPE Annual TechnicalConference and Exhibition, San Antonio, Texas, USA, 29 September–2 October. DOI: 10.2118/77724-MS.
Solano, R., Johns, R.T., and Lake, L.W. 2001. Impact of Reservoir Mixing on Recovery in Enriched-Gas Drives Above the Minimum Miscibility Enrichment. *SPEREE* **4** (5): 358–365. SPE-73829-PA. DOI: 10.2118/73829-PA.
Stalkup, F. 1998. Predicting the Effect of Continued Gas Enrichment Above the MME on Oil Recovery in Enriched Hydrocarbon Gas Floods. Paper SPE 48949 prepared for presentation at the SPE Annual Technical Conference and Exhibition, New Orleans, 27–30 September. DOI: 10.2118/48949-MS.
Streamsim Technologies. 2004. San Francisco, www.streamsim.com.
Todd, M.R. and Chase, C.A. 1979. A Numerical Simulator for Predicting Chemical Flood Performance. Paper SPE 7689 presented at the SPE Reservoir Simulation Symposium, Denver, 31 January–2 February. DOI: 10.2118/7689-MS.
Tomich, J.F., Dalton, R.L. Jr., Deans, H.A., and Shallenberger, L.K. 1973. Single-Well Tracer Method to Measure Residual Oil Saturation. *JPT* **25** (2): 211–218; *Trans.,* AIME, **255.** SPE-3792-PA. DOI: 10.2118/3792-PA.
UTCHEM-7.0—A Three-Dimensional Chemical Flood Simulator. 1998. Technical Documentation, Vol. 2, Reservoir Engineering Research Program, Center for Petroleum and Geosystems Engineering, University of Texas at Austin, Austin, Texas.
Warren, J.E. and Skiba, F.F. 1964. Macroscopic Dispersion. *SPEJ* **4** (3): 215–230; *Trans.,* AIME, **231.** SPE-648-PA. DOI: 10.2118/648-PA.
Wellington, S.L., Simmone, J.F., Hara, S.K., and Richardson, E.A. 1994. A Single Well Test Method That Yields a Dispersion-Free Measure of Reservoir Fluid Drift Rate. Paper SPE 27757 presented at the SPE/DOE Improved Oil Recovery Symposium, Tulsa, 17–20 April. DOI: 10.2118/27757-MS.

Appendix

Additive Dispersivities. Warren and Skiba (1964) refered to earlier work in stating an additive dispersivity principle: The apparent or observed dispersivity is the sum of dispersivities of statistically independent simultaneously acting processes. We express that principle as

$$\alpha_a \approx \alpha + \alpha_{ac}, \qquad \text{(A-1)}$$

where α_{ac} is apparent dispersivity resulting from conformance alone (α=0) and is shown by numerous examples in the paper to be linearly scale-dependent. We reached the following conclusions independent of scale, on the basis of simulations that use the Muskat equation (Eq. 12), then fitting the generated $C(Q_D)$ results to the C/D equation (Eq. 3). We found Eq. A-1 to be very accurate. We also found:

$$\alpha_{ac} \approx \alpha_{ap} + \alpha_{as}, \qquad \text{(A-2)}$$

where α_{ap} is the apparent dispersivity owing only to areal pattern conformance and α_{as} is the apparent dispersivity owing only to stratification (vertical) conformance, in agreement with Muskat (1949) .

At field scale, for all practical purposes $\alpha_{ac}>>\alpha$, leading to the important observation

$$\alpha_a \approx \alpha_{ac}, \qquad \text{(A-3)}$$

with the consequence that $\alpha_a \approx \alpha_{ap} + \alpha_{as}$.

***Apparent Dispersivities of Laboratory Core Plugs*.** Laboratory dispersivity values are obtained from coreflood effluent profiles by use of Eq. 3, or another best-fit procedure, to obtain apparent dispersivity α_a. If the core were homogeneous, then α_a would equal the physical dispersivity, α, corresponding to its microscale heterogeneity. Because any core will have some heterogeneity, the effluent profile and its associated α_a will reflect the combined effects of physical dispersivity and heterogeneity. Let α_{ac} denote the dispersivity resulting from conformance (heterogeneity) alone (no dispersion, α=0) and let α denote the physical dispersivity (no heterogeneity). Are the dispersivities additive?

We address this question by use of a stratified model and the Muskat solution with F given by the C/D equation (Eq. 3). Let $k(z)$ be described by Eq. 11, with V=0.13, and assume physical dispersivity α=0.01 ft. The purely dispersive profile of Eq. 3 for α=0.01 ft is given by a Peclet number $N_{\text{Pe}}=L/\alpha=100$ (by use of L=1 ft). By use of the Muskat solution (Eq. 12) for V=0.13—where $F(Q_D)$ is a step function, C=0 for Q_D<1, and C=1 for $Q_D \geq 1$, corresponding to α=0—we obtain a Peclet number $N_{\text{Pe}ac}$=103 from Eq. 3. By use of the Muskat solution with V=0.13 and $F(Q_D)=C$ from Eq. 3 with α=0.01, we obtain the solution reflecting the combined, simultaneously acting effects of heterogeneity and dispersion; the apparent Peclet number N_{Pe} is 50.6. Eq. A-1 is equivalent to

$$N_{\text{Pe}a}^{-1} = N_{\text{Pe}ac}^{-1} + N_{\text{Pe}}^{-1} \qquad \text{(A-4)}$$

because $N_{\text{Pe}}^{-1}$is α/L, and L cancels out. The above Peclet numbers give:

$$N_{\text{Pe}a}^{-1} = 0.01977 = N_{\text{Pe}a}^{-1} + N_{\text{Pe}}^{-1} = 0.00974 + 0.01 = 0.01974$$

affirming Eq. A-1. The same analysis is used for a more heterogeneous V=0.4. The three respective Peclet numbers, N_{Pe}=100, $N_{\text{Pe}ac}$=7.397, and $N_{\text{Pe}a}$=6.839 used in Eq. A-1 yield:

$$N_{Pe\alpha}^{-1} = 0.1462 = N_{Pe\alpha c}^{-1} + N_{Pe}^{-1} = 0.1352 + 0.01 = 0.1452$$

again affirming Eq. A-1. The coreflood-profile Peclet number $N_{Pe\alpha}$ =6.839 gives an apparent dispersivity (if L=1 ft) of α_a=0.1462 ft, approximately 15 times larger than the physical dispersivity. In view of Eq. A-1, perhaps the only definitive statement regarding differences between laboratory and physical dispersivity is that physical dispersivity is no larger than laboratory dispersivity.

Additive Conformance Dispersivities. By use of the same approach described in the previous section for showing how physical and stratification dispersivities are additive, a similar exercise was conducted to test if areal pattern and stratification dispersivities are also additive, as stated by Muskat (1949).

Consider again the results shown in Fig. 7 and discussed in the Stratified Five-Spot subsection. The open black circles connected with a thin black line represent apparent Peclet numbers estimated by use of additive conformance dispersivities from Eq. A-2 for a wide range of stratification, from V=0 to 0.9. The stratified five spot $C(Q_D)$ from the Muskat solution gives the combined, simultaneously acting effects of areal pattern conformance and stratification (vertical) conformance. Fitting this solution to the 1D C/D equation (Eq. 3) yields the apparent Peclet numbers shown as a solid black line in Fig. 7. The maximum error in estimated apparent Peclet number by use of additive dispersivities is 7% and is exact for V=0.

SI Metric Conversion Factors

ft × 3.048*	E − 01 = m
ft^2 × 9.290 304*	E − 02 = m^2
ft^3 × 2.831 685	E − 02 = m^3
in. × 2.54*	E + 00 = cm
psi × 6.894 757	E − 00 = kPa

*Conversion factor is exact.

Keith H. Coats is Technical Director of Coats Engineering, Inc. in Marco Island, Florida, specializing in development of reservoir simulation software. He previously worked in simulation-software development for Intercomp in Houston. Coats holds BS, MS, and PhD degrees in chemical engineering and an MS degree in mathematics, all from the University of Michigan. He has served as an SPE Distinguished Lecturer and is a recipient of the 1984 Lester C. Uren award and 1988 Anthony F. Lucas Gold Medal. He was elected to the National Academy of Engineering in 1988 and was selected by Hart's E&P as one of the 100 most influential people of the petroleum century in March 2000. **Curtis H. Whitson** is a professor of petroleum engineering and applied geophysics at the Norwegian U. of Science and Technology (NTNU) in Trondheim. E-mail: curtis.h.whitson@ntnu.no. He is also the founder of PERA, a consulting company specializing in compositionally sensitive reservoir processes. Whitson holds a BS degree in petroleum engineering from Stanford U. and a PhD (dr.techn.) degree from the Norwegian Inst. of Technology (NTH, now NTNU). He has authored a number of publications on phase behavior, gas condensates, well performance, and enhanced oil recovery and is coauthor of the SPE monograph Phase Behavior. **L. Kent Thomas** is currently an independent consultant following retirement from the Upstream Technology Division of ConocoPhillips in 2006. E-mail: lktkent@swbell.net. He holds a BS degree from the University of Oklahoma and MS and PhD degrees from the University of Michigan, all in chemical engineering. Thomas is a Distinguished Member of SPE and the recipient of the 1993 Reservoir Engineering Award and the 2002 Robert Earll McConnell Award from AIME. Thomas has held positions on numerous SPE reservoir engineering committees, including Technical Program Chairperson for the Annual Technical Conference and Exhibition, Chairperson of the Forum Series Coordinating Committee, Chairperson of the Forum Series Committee on Naturally Fractured Reservoirs, Chairperson of the SPE Symposium on Reservoir Simulation and on the SPE Textbook Committee. Thomas also has served as a Distinguished Lecturer and as an SPE instructor on Reservoir Simulation.